

CHAPTER 3A

***Oreocnide integrifolia* (Gaud.) miq can alleviate high fat diet induced derangement in carbohydrate metabolism in type 2 diabetic C57BL/6J mouse model.**

Introduction:-

India has recorded the greatest increase in the number of diabetic subjects in recent times and, with a current prevalence of 2.4% in the rural population and 11.6% in the urban population, it is estimated that by 2025, India will be world leader (King *et al.*, 1998, Tripathi & Srivastava, 2006). Though many drugs are commercially available for treating the disease, most of them are out of reach for many and are also beset with some adverse effects (Sharma *et al.*, 2008). Treatments are essentially aimed at controlling hyperglycemia, which includes insulin secretagogues (Sulphonylureas, meglitinides, GLP analogues) and insulin sensitizers which reduce hepatic glucose generation (Metformin) or enhance peripheral glucose uptake by muscle and adipose tissue (Metformin, thiazolidinediones) but, no drug in vogue intrinsically exerts both the effects (Tousch *et al.*, 2008). The use of medicinal herbs in this context is a meaningful alternative and in recognition this fact, WHO has advised research in this direction and affirmed that, traditional plant based treatments for diabetes warrants further attention (WHO, 1980).

Oreocnide integrifolia (Gaud.) Miq (family Urticaceae) are shrubs/small trees mainly distributed in India, China, Bhutan, Indonesia, Laos, Myanmar, Sikkim and Thailand (Chen *et al.*, 2003). They are also cooked and eaten for maintaining normal blood pressure levels by people of Manipur (Singh *et al.*, 2000). The roots of *Oreocnide integrifolia* are mixed with ginger powder and applied for treatment of

rashes by Khasi and Jaintia tribes of Meghalaya (Kharkongor & Joseph, 1981; Begum & Nath, 2000) and an infusion prepared from the leaves is used as a decoction to alleviate diabetic symptoms. Type 2 Diabetes mellitus is a metabolic disease with a plethora of heterogeneous interrelated manifestations and complications like hyperglycemia, hyperinsulinemia, insulin resistance, impaired glucose tolerance and peripheral utilization, decreased hepatic glycolysis, increased gluconeogenesis, dyslipidemia etc, all of which are related primarily with insulin and its action. Chronic hyperglycemia caused due to abnormalities in glucose metabolism and insulin resistance characterizes Type 2 Diabetes (Kim *et al.*, 2000). Increased hepatic and plasma free fatty acids in consequence to high fat diet, are characteristic of diabetic subjects. The higher serum free fatty acid levels lower the ability of insulin to suppress hepatic glucose production by activating gluconeogenesis and inhibiting glycolysis (Shah *et al.*, 2003, Kishore *et al.*, 2006). All these metabolic alterations associated with Type 2 Diabetes result from a relative insufficiency of insulin to overcome peripheral insulin resistance. A set of health problems like hyperlipidemia, atherosclerosis and hypertension linked to impaired carbohydrate and lipid metabolisms are all consequences of both insulin deficiency and resistance (Brosche, 2001; Jayaprakasam *et al.*, 2006). Any antidiabetic agent should exert ameliorative effect on the diabetic manifestations by enhancing insulin secretion and/or by improving /mimicking insulin action. Despite the existing treatment modalities, there is need for new treatment paradigms for Type 2 Diabetes to control the progressive metabolic deterioration (Turner *et al.*, 1999). Alternative agents being explored should be able to hit at the sites of basic defects alluded to the disease, which are essentially islet dysfunction in association with insulin resistance. Molecular mechanisms underlying these basic defects also need to be evaluated to have a better

understanding. To facilitate such evaluations, appropriate clinically relevant experimental model is required. The C57BL/6J mice when fed with high fat diet develops all classical Type 2 Diabetic symptoms like insulin resistance and insufficient islet compensation, and hence serves as an ideal model for studying pathophysiology of impaired glucose tolerance and Type 2 Diabetic manifestations at molecular level (Ahren *et al.*, 1997; Ahren & Pacini 2002; Reimer *et al.*, 2002; Pripic *et al.*, 2003; Winzel *et al.*, 2003). This mouse also serves as a good model for evaluating the efficacy of new antidiabetic agents as well (Ahren *et al.*, 1999; Ahren *et al.*, 2000a, b). Natural products from medicinal plants are of focal interest in the discovery of new chemical entities in modern drug discovery programs. It is in this context, that we had initiated studies on *Oreocnide integrifolia* (Gaud.) Miq (OI) used by people in north eastern part of India. Previously, we had demonstrated potent antihyperglycemic and antihyperlipidemic effects of OI leaf extract in a dose and duration dependent manner in streptozotocin induced diabetic rats (Ansarullah *et al.*, 2009). So, the present study was planned to evaluate the antihyperglycemic action and mechanism of glucoregulation of OI extract, when supplemented with simultaneous to high fat diet.

Materials & Methods:

Animals and Diets: Male C57BL/6J mice (age 4-5 weeks) were procured from National Centre for Laboratory Animal Service, National Institute of Nutrition, Hyderabad, India. To make a fully developed insulin resistant diet induced obese (DIO) animal phenotype, 20 animals were fed with high-fat diet (60 kcal% fat, D12492 Research Diet, New Brunswick, NJ), 20 were fed with high fat diet

supplemented (mixed with feed) with 3% O.I extract and another 20 were maintained on standard laboratory diet for 24 weeks. The experiment was carried out according to the guidelines of the Committee for the Purpose of Control and Supervision of Experiments on Animals India, and approved by the Animal Ethical Committee of the Department of Zoology, The M.S University of Baroda, Vadodara (Approval No. 827/ac/04/ CPCSEA).

Tissue glycogen content: At the end of experimentation, animals were sacrificed under anesthesia and liver and muscle were taken out for evaluation of various parameters. Liver and muscle glycogen contents were estimated by the method of Seifter *et al.* (1950).

Plasma Glucose and Insulin: Plasma glucose was measured by tail snipping method using One Touch Glucometer (Elegance, USA). Plasma Insulin was quantified using Mouse Insulin ELISA kit (Merckodia Diagnostics, Uppsala, Sweden).

Glucose Tolerance Test (GTT) & Insulin Response Test (IRT): On the days of the test, a subset (n=6) of animals was fasted for 12 h followed by an intraperitoneal administration of glucose (2g/kg). Blood glucose levels were determined in blood samples from the tail vein at 0 (prior to glucose administration), 30, 60, 90 and 120 min after glucose administration. For Insulin response test, another subset (n=6) of animals was administered with 0.2 IU of Insulin intraperitoneally (Human Insulin, Lantus, Aventis Pharma GmbH, Germany) and blood glucose was determined at different time points as described above. The results are expressed as integrated area under the curve (AUC) for glucose and insulin, calculated by the trapezoid rule [AUC = $(C_1 + C_2) / 2 \times (t_1 - t_2)$] and changes in glucose concentrations during OGTT and ITT are expressed as AUC_{glucose} (mg/dl per min).

[¹⁴C] Glucose Oxidation: Radiolabelled [¹⁴C] was procured from Board of Radiation and Isotope Technology (BRIT), Mumbai, India. [¹⁴C] Glucose oxidation in gastrocnemius muscle and liver was estimated by the method of Johnson and Turner (1972). Briefly, 10mg of tissue was placed in a 2 ml ampoule containing 170 µl DMEM (pH 7.4), 10 U penicillin in 10 µl DMEM and 0.5 µCi [¹⁴C]-glucose. After aeration with gas mixture (5% CO₂ and 95% air) for 30s, the ampoule was tightly closed with rubber cork and 100 µl of Diethanolamine (pH-9.5) buffer was applied to filter paper before closing the ampoule. This closed system with CO₂ trap was incubated at 37 °C. The CO₂ traps were replaced every 2 h and 100 µl of 1 N H₂SO₄ was added to the ampoule upon the removal of second trap to halt further metabolism and release of any residual CO₂ from the sample. The ampoule was again closed for 1 h before the third and final trap was removed and all the CO₂ traps were placed in the scintillation vials containing 10 ml of scintillation fluid [2,5-diphenyloxazole and 1,4-bis(5-phenyloxazole 2-yl) in scintillation grade toluene] and counted for ¹⁴C radioactivity in a Packard scintillation beta counter. Results are expressed as CPM of ¹⁴CO₂ released/10mg tissue.

RNA isolation and RT-PCR:

RNA isolation

RNA was isolated from the tissues by the method of Chomczynski and Sacchi, 1987

1) Trizol method

i. Homogenization:

Approximately, 50-100 mg of tissue sample was homogenized in 1 ml of TRIZOL® Reagent (Invitrogen, USA) using a glass-Teflon® homogenizer. The sample volume was not exceeded 10% of the volume of

TRIZOL® Reagent used for homogenization. Insoluble material from the homogenate was removed by centrifugation at $12,000 \times g$ for 10 minutes at 2 to 8°C. The resulting pellet contained extracellular membranes, polysaccharides, and high molecular weight DNA, while the supernatant contained RNA. In samples from fat tissue, an excess of fat collects as a top layer which was removed from the tube.

ii. Phase separation:

Homogenized samples were incubated for 5 min at 15-30 °C to permit the complete dissociation of nucleoprotein complexes. About 0.2 ml of chloroform per ml of Trizol reagent was added, mixed vigorously for 15 sec and incubated it at 15-30 °C for 2-3 min. which was further centrifuged at 12,000 g for 15 min at 2-8 °C. Following centrifugation, the mixture separated into a lower red, phenol-chloroform phase, an interphase, and a colorless upper aqueous phase. RNA remained exclusively in the aqueous phase. The volume of the aqueous phase was about 60% of the volume of TRIZOL® Reagent used for homogenization. The aqueous phase was transferred to a fresh tube (uppermost aqueous phase).

iii. RNA precipitation and wash:

Around 0.5 ml of isopropyl alcohol was added to the aqueous phase and incubated at 15-30 °C for 10 min and centrifuged at 12,000 g for 10 min at 2-8 °C. The supernatant was removed and pellet was washed with (1 ml) 75% ethanol. The tubes were vortexed and centrifuged at 7500 g for 5 min at 2-8 °C. The supernatant was removed and the RNA pellet was allowed to air dry. Further, 50 µl DEPC treated water was added to dissolve the RNA

pellet and incubated at 55-60 °C for 5-10 min. RNA was stored at -20 °C / -70 °C until used.

iv. DNase Treatment:

5 µl 20x DNase buffer and 8 units of RNase free-DNase was added and incubated at 37 °C for 30 min. To this 20ul of DNase inactivation reagent was added supplied with the kit [Ambion Inc., 2007] and mixed thoroughly. This was incubated at RT for 2 min and centrifuged at 16, 000 g for 1 min. The RNA solution was transferred to new RNase free tube and stored at -80°C.

v. Purity and concentration of RNA:

The quality of RNA was checked spectrophotometrically at 260 and 280 nm and run on 1.5% agarose gel electrophoresis before proceeding for cDNA synthesis. RNA samples having ratio of $A_{260/280}$; greater than 1.8 were used for cDNA synthesis.

Agarose Gel Electrophoresis for RNA:

Materials

10X MOPS buffer

0.4 M MOPS, pH 7.0

0.1 M sodium acetate

0.01 M EDTA

Agarose (1.5 g), Bromo phenol blue (BPB), Ethidium Bromide (EtBr)

(All reagents were prepared in DEPC treated water)

Method

1.5 g agarose was added to 100 ml 1x MOPS buffer and boiled. To this added 2 ul of EtBr (2mg/ml) and mixed thoroughly. The gel was casted and 5ul of total RNA was loaded with bromo phenol blue. Electrophoresis was carried out and visualized the gel on a UV transilluminator.

First Strand cDNA synthesis

First strand cDNA synthesis was done according to the manufacturer's instructions by the kit method (High-Capacity cDNA Reverse Transcription Kit) Applied Biosystems, Foster City, CA, USA.

Briefly, 10 μ l (3 ug) of total RNA was taken and added 1ul (0.5ug) of Oligo (dT)₁₈ primer, mixed gently and spin down for 3-5 sec at 3000 g. Incubated at 70 °C for 5 min and kept it on chilled ice and spin down by brief centrifugation (for 3-5 sec at 3000 g). Added 5X reaction buffer (4ul); Ribonuclease inhibitor 1ul (20U); 10mM dNTPs (2ul) and mixed gently and spin down for 3-5 sec at 3000 g. Incubated at 37 °C for 5 min. Then, added M-MuLV Reverse Transcriptase 2ul (40U). Incubated the reaction mixture at 37 °C for 60 min. Stopped the reaction by incubating it at 70 °C for 10 min and stored this at -20 °C.

Second Strand cDNA synthesis:

Second strand cDNA synthesis was carried out by Taq polymerase [Bangalore Genei] according to manufacturer's instructions.

2 μ l (1ug) of first strand cDNA was taken and specific primers (forward and reverse; 1ul (10pmoles) were added for amplification of genes such as Glucokinase, Glucose-6-phosphatase, Phosphoenolpyruvate-carboxykinase and Beta-actin (house

keeping gene) About 2 ul (2.5mM) dNTPs; 10X Taq buffer 2ul; Taq polymerase 0.333ul (1U) and made up the volume to 20ul by nuclease free water.

List of primer sequences used for amplification of target genes.

Sr.no	Gene of Interest	Primer sequence 5'-3'	Tm°C
1	Glucokinase (Amplicon size:490bp)	Sense : TTCACCTTCTCCTTCCCTGTAAGGC Antisense: TACCAGCTTGAGCAGCACAAGTCG	64
2	Glucose-6-phosphatase (Amplicon size :607bp)	Sense : AAGACTCCCAGGACTGGTTCATCC Antisense: TAGCAGGTAGAATCCAAGCGCG	63
3	Phosphoenolpyruvate-carboxykinase (Amplicon size:489bp)	Sense : TGCTGATCCTGGGCATAACTAACC Antisense: TGGGTACTCCTTCTGGAGATTCCC	62
4	Beta-Actin (Amplicon size: 240bp)	Sense : TCACCCACACTGTGCCCCATCTACGA Antisense: CAGCGGAACCGCTCATTGCCAATGG	60

The PCR conditions were set up as follows:

Initial Denaturation	94 °C for 5 min
Denaturation	94 °C for 30 sec
Annealing	58-62 °C for 30 sec
Extension	72 °C for 30 sec
	35 cycles
Final Extension	72 °C for 10 min
Hold at 22 °C	

Confirmation of second strand cDNA:

The second strand cDNA for various genes were confirmed on 2 % agarose gel electrophoresis.

Agarose Gel Electrophoresis for DNA:

Materials

50X TAE buffer (pH 8.0)

Tris Base - 24.2 g

Glacial Acetic acid - 5.71 ml

0.5m EDTA - 10 ml

Agarose, Bromo phenol blue (BPB), Ethidium Bromide (EtBr)

(All reagents were prepared in double distilled autoclaved water)

Method: Appropriate quantities of agarose for various percentage gels were weighed and added in 100 ml 1x TAE buffer and boiled. To this, 2 ul of Ethidium Bromide (2mg/ml) was added and mixed thoroughly. The gel was casted and 2 ul of DNA was loaded with bromophenol blue. Electrophoresis was carried out and visualized the gel on a UV transilluminator. A 100 base pair DNA ladder (Fermentas, Canada) was also run along with pcr products to confirm the size of amplicons.

Then the gels were subjected to densitometric scanning (Alpha Imager Gel Doc) to determine the optical density of each band and then normalized against β -actin with help of Image J, Software NIH, USA.

Statistical analysis: Statistical evaluation of the data was done by one way ANOVA followed by Bonferroni's Multiple comparison test .The results are expressed as mean \pm S.E using Graph Pad Prism version 3.0 for Windows, Graph Pad Software, San Diego, California USA.

RESULTS:

Glycogen content: High fat diet feeding caused significant ($P < 0.001$) depletion of hepatic glycogen content to the tune of 41% while, supplementation with OI extract minimized it to 20% (Fig. 1, 2). However, the decrease in muscle glycogen content seen in diabetic animals was prevented near completely with simultaneous supplementation with OI extract.

Plasma glucose level and insulin titre (Table 1; Fig. 3, 4): Plasma glucose level (Fig. 3) was increased by 64% in high fat diet mice compared to controls (5.70 ± 0.71 Vs 16.12 ± 0.81 mmol/L) at the end of 24 weeks (Table 1). OI extract supplementation along with high fat diet resulted in only 20% increase in plasma glucose level. The plasma insulin titre (Fig. 4) decreased in high fat diet fed diabetic mice, while simultaneous supplementation with OI extract showed a non-significant change.

Glucose tolerance and insulin response tests (Fig. 5-8): Administration of 2.0g glucose/kg body weight to normal and diabetic mice raised plasma glucose levels from 5.58 to 11.43 and 15.74 to 27.01mmol/l respectively by 30 minutes while, in OI extract supplemented group, the rise in glucose level at the same time was, 13.73 from 9.01 mmol/l (Fig 5). The diabetic mice displayed marked glucose intolerance compared to controls as corroborated by the AUC_{glucose} values (Fig 6). OI extract supplemented mice showed better glucose clearance compared to that of diabetic mice. Furthermore, diabetic mice displayed higher glycemic status even at the end of

90 min of insulin administration compared to controls (Fig 7). OI extract supplemented mice started recovery of glycemic level by 60 min of insulin loading itself from 4.87 to 5.72 mg/dl and showed decreased AUC_{glucose} value as compared to diabetic animals (Fig 8).

[¹⁴C] Glucose oxidation: High fat diet feeding caused a remarkable decrease ($P < 0.001$) in hepatic (1876.7 ± 86.3 Vs 976.3 ± 87.75) (Fig. 9) and muscle (1475.3 ± 56.77 Vs 732.5 ± 88.32) glucose oxidation rates as compared to normal diet fed animals (Fig 10). Glucose oxidation rate was maintained better by OI extract supplementation in both liver and muscle when compared with diabetic mice at the end of 24 weeks of treatment period.

Expression of gluco-regulatory enzymes: The hepatic enzyme markers of gluco-regulation were studied using semi-quantitative RT-PCR. Glucokinase expression was found to be decreased significantly ($P < 0.001$) by 3 fold when fed with high fat diet compared to normal chow feeding (Fig 11). However, G-6-Pase and PEPCK mRNA expressions recorded significant increase (Fig 12 & 13). Supplementation with OI extract effectively prevented these changes in glucokinase, G-6-Pase and PEPCK expressions.

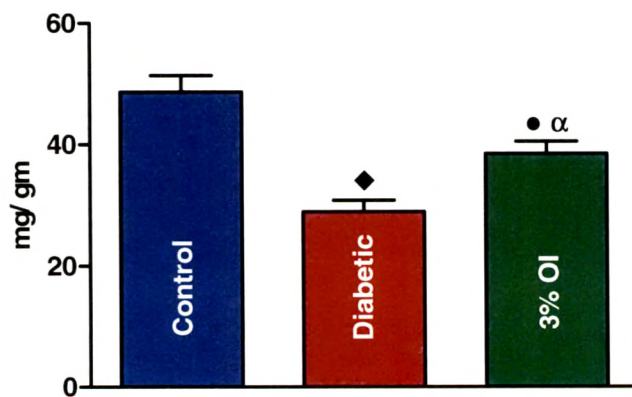
Table 1. Plasma glucose and insulin levels in control and experimental animals.

	Control	Diabetic	OI treated
Glucose mmol/L	5.70± 0.71	16.12± 0.81 [♦]	8.90 ± 0.56 ^{•δ}
Insulin pmol/L	88.32 ±7.27	66.39 ± 6.63 [•]	72.43 ±10.25

●= p<0.01, ■=p<0.001, ♦=p<0.0001: Experimental groups compared to control

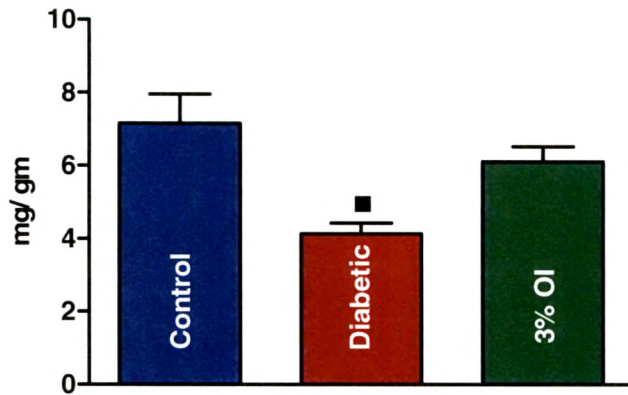
α= p<0.01, β= p<0.001, δ= p<0.0001: OI treated group compared to diabetic group

Fig. 1. Effect of 3% OI extract on hepatic glycogen content in control and experimental animals



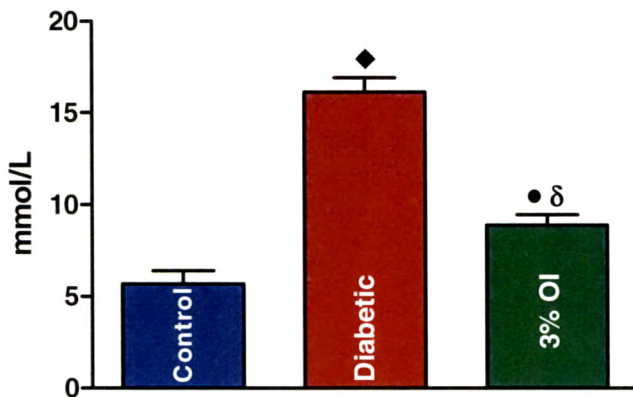
●=p<0.01, ■=p<0.001, ♦=p<0.0001: Experimental groups compared to control group
 α=p<0.01, β=p<0.001, δ=p<0.0001: OI treated group compared to diabetic group

Fig. 2. Effect of 3% OI extract on muscle glycogen content in control and experimental animals



●=p<0.01, ■=p<0.001, ◆=p<0.0001: Experimental groups compared to control group

Fig. 3. Effect of 3% OI extract on plasma Glucose level in control and experimental animals



●=p<0.01, ■=p<0.001, ◆=p<0.0001: Experimental groups compared to control group
α=p<0.01, β=p<0.001, δ=p<0.0001: OI treated group compared to diabetic group

Fig. 4. Effect of 3% OI extract on Plasma Insulin level in Control and Experimental animals

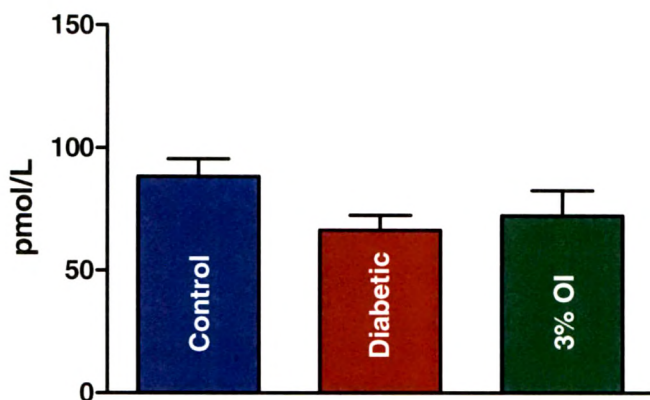
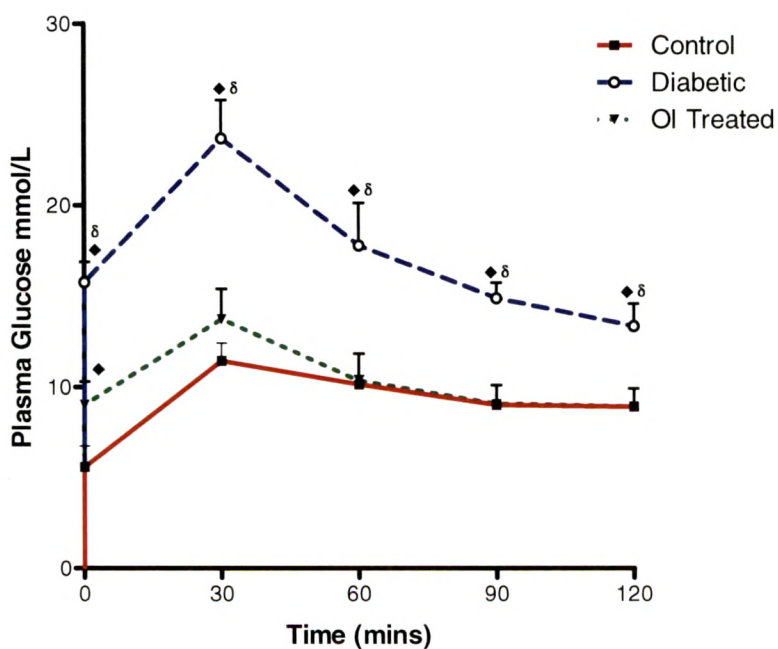
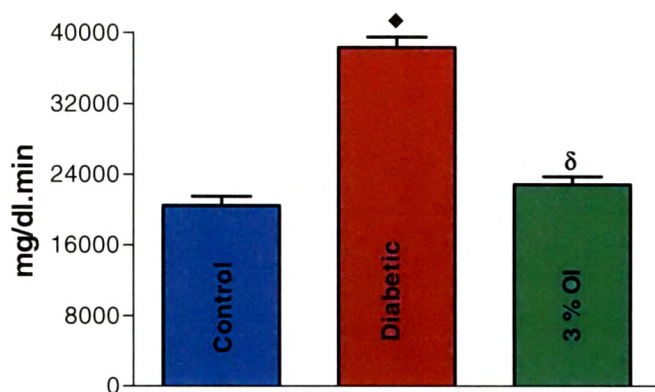


Fig. 5. Effect of 3% OI extract on Intraperitoneal Glucose Tolerance test



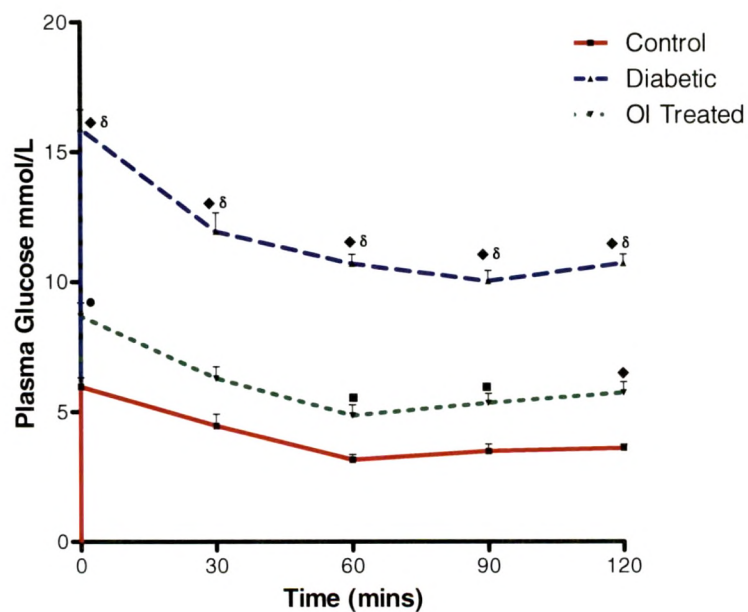
●=p<0.01, ■=p<0.001, ◆=p<0.0001: Experimental groups compared to control
 α=p<0.01, β=p<0.001, δ=p<0.0001: 3% OI treated group compared with diabetic group

Fig. 6. Effect of 3% OI extract on OGTT in control and experimental animals (Expressed as AUC + SEM)



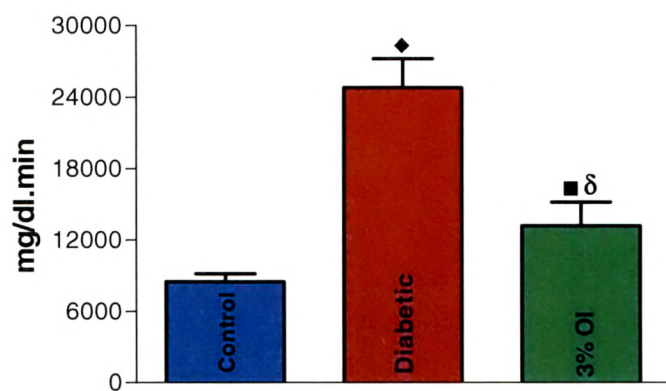
●=p<0.01, ■=p<0.001, ◆=p<0.0001: Experimental groups compared to control group
 α=p<0.01, β=p<0.001, δ=p<0.0001: OI treated group compared to diabetic group

Fig. 7. Effect of 3% OI extract on Intraperitoneal Insulin Response test



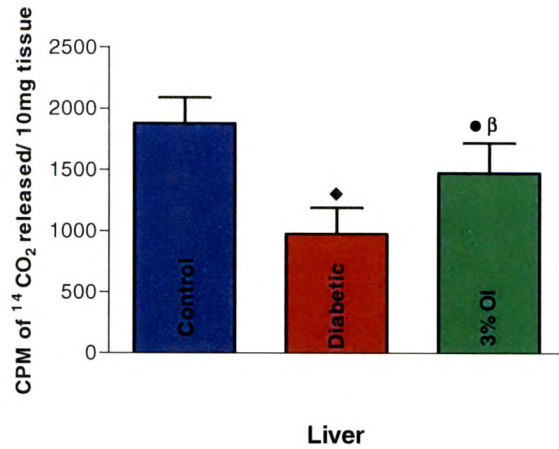
●=p<0.01, ■=p<0.001, ◆=p<0.0001: Experimental groups compared to control
 α=p<0.01, β=p<0.001, δ=p<0.0001: 3% OI treated group compared with diabetic group

Fig. 8. Effect of 3% OI extract on IRTT in control and experimental animals (expressed as AUC + SEM)



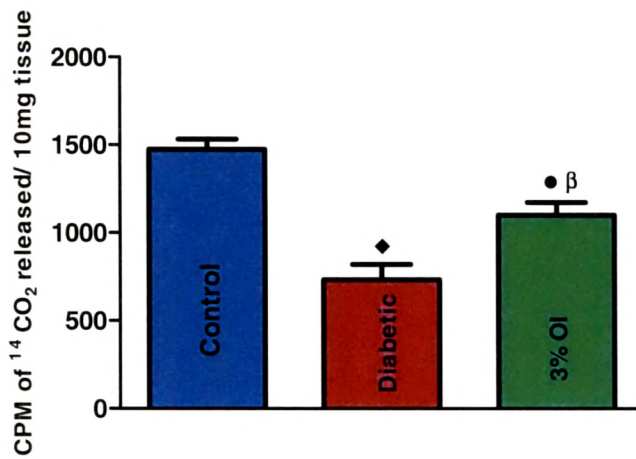
•=p<0.01, ■=p<0.001, ◆=p<0.0001: Experimental groups compared to control group
α=p<0.01, β=p<0.001, δ=p<0.0001: OI treated group compared to diabetic group

Fig. 9. Effect of 3% OI extract on ^{14}C liver glucose oxidation rates in control and experimental animals



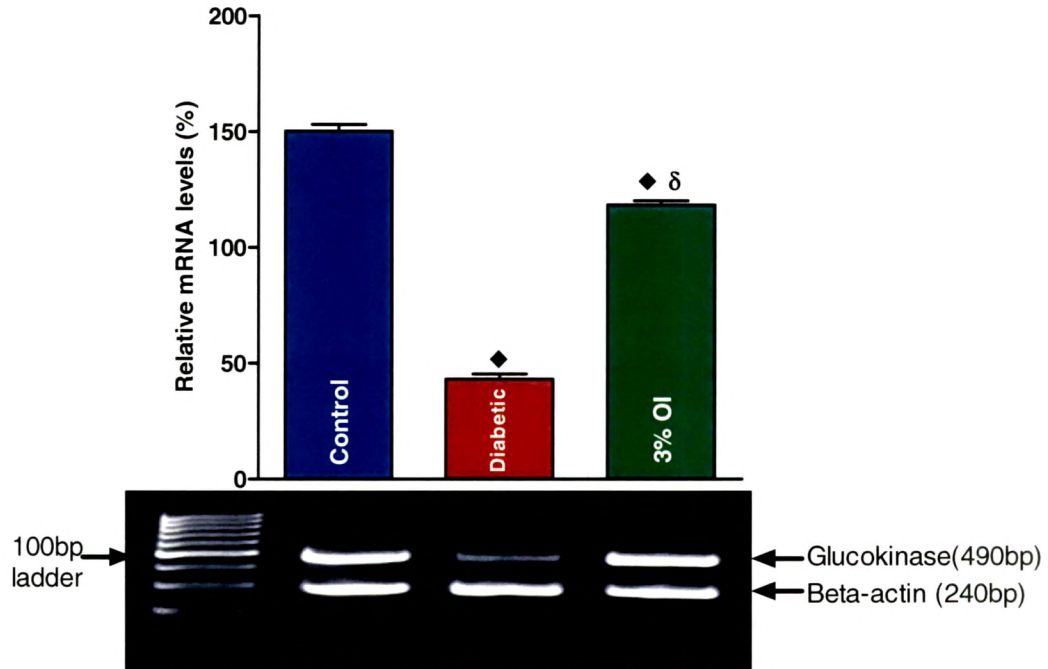
●=p<0.01, ■=p<0.001, ◆=p<0.0001: Experimental groups compared to control group
 α =p<0.01, β =p<0.001, δ =p<0.0001: OI treated group compared to diabetic group

Fig. 10. Effect of 3% OI extract on ^{14}C muscle glucose oxidation rates in control and experimental animals



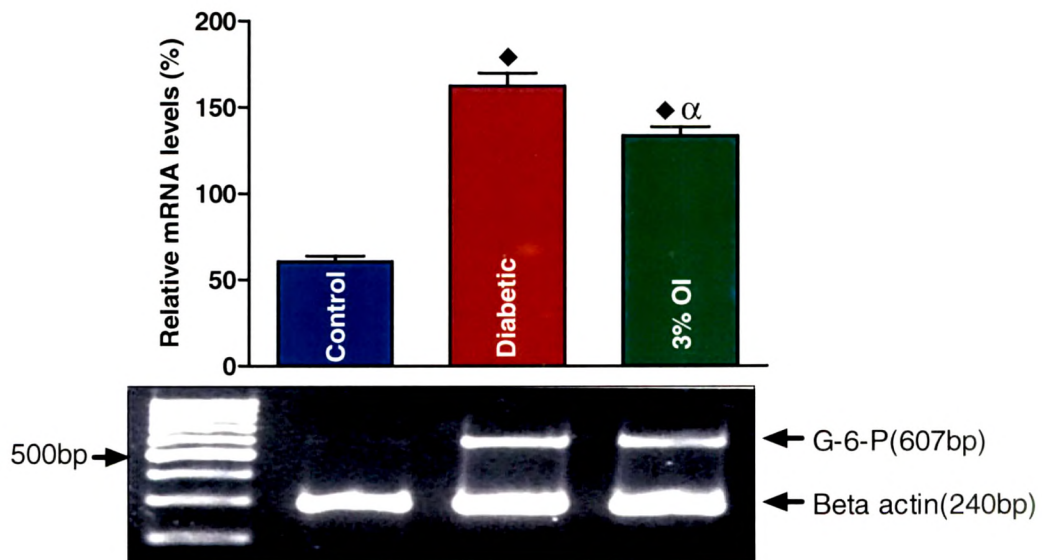
●=p<0.01, ■=p<0.001, ◆=p<0.0001: Experimental groups compared to control group
 α =p<0.01, β =p<0.001, δ =p<0.0001: OI treated group compared to diabetic group

Fig. 11. Effect of 3% OI extract on Hepatic Glucokinase expression in control and experimental animals



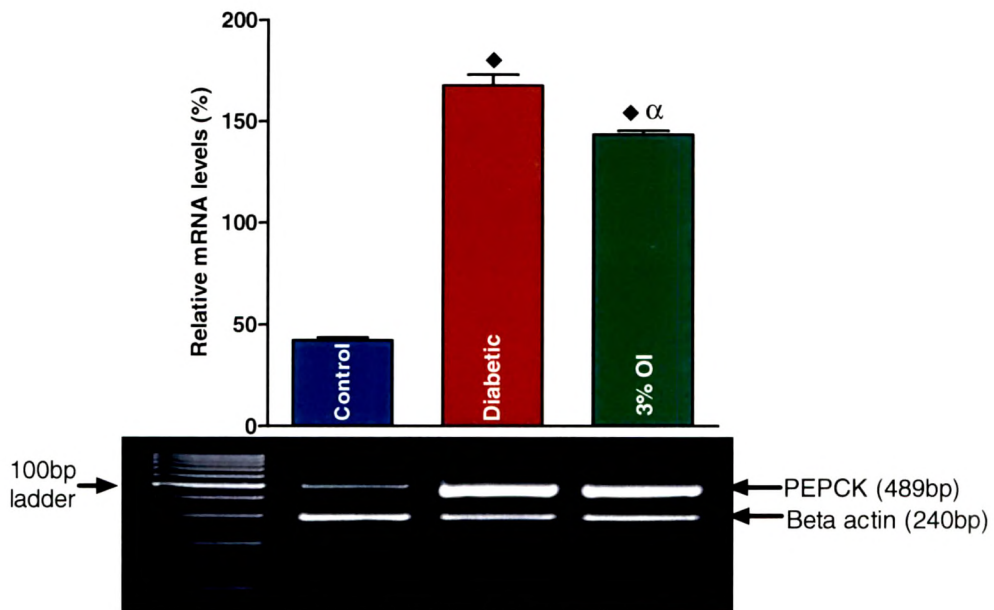
●=p<0.01, ■=p<0.001, ◆=p<0.0001: Experimental groups compared to control group
α=p<0.01, β=p<0.001, δ=p<0.0001: OI treated group compared to diabetic group

Fig. 12. Effect of 3% OI extract on glucose-6-phosphatase expression in control and experimental animals



●=p<0.01, ■=p<0.001, ◆=p<0.0001: Experimental groups compared to control group
 α=p<0.01, β=p<0.001, δ=p<0.0001: OI treated group compared to diabetic group

Fig. 13. Effect of 3% OI extract on Hepatic PEPCK expression in control and experimental animals



●=p<0.01, ■=p<0.001, ◆=p<0.0001: Experimental groups compared to control group
α=p<0.01, β=p<0.001, δ=p<0.0001: OI treated group compared to diabetic group

Discussion:

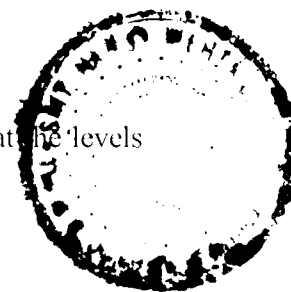
The study has tried to evaluate the efficacy of OI extract as a protectant against high fat diet induced type 2 diabetic C57BL6/J mouse model. The high fat diet fed C57BL6/J mouse is a robust and efficient model not only for studying the mechanics of progressive development of impaired glucose tolerance (IGT) and insulin resistance (IR) leading to Type 2 Diabetes, but also for developing novel therapeutic interventions (Winzell and Ahren, 2004). This mouse model shows slightly different time schedules of stages of development of insulin resistance and type-2 diabetes, probably based on maintenance conditions and adaptations on a global scale. The present model maintained in India apparently reaches the IGT and IR stage by 8-10 weeks on high fat diet and type 2 diabetic stage with islet dysfunction by 18-20 weeks, as characterized by our preliminary studies. The present study was essentially undertaken to evaluate the efficacy of OI extract on glucose dyshomeostasis, when given continuously for 24 weeks simultaneous to high fat diet. By 24 weeks, high fat diet alone fed group of mice showed type-2 diabetic manifestations marked by hyperglycemia to the tune of 200%, hypoinsulinemia to the extent of 20% and an altered higher level of glucose homeostasis and insulin sensitivity as recorded by the glycemic changes during glucose tolerance and insulin response tests (GTT and IRT). Attendant metabolic alterations are manifest in the form of reduced peripheral glucose oxidation and hepatic glucokinase mRNA expression, coupled with increased hepatic glucose-6-phosphatase and phosphoenol pyruvate carboxykinase mRNA expressions. Clearly, by 24 weeks of high fat diet, the C57BL/6J mice develop type 2 diabetic manifestations and hence are an excellent model to evaluate the efficacy of therapeutic agents for human type-2 diabetes induced hyperglycemia. Many other investigators have also reported development of

insulin resistance and type-2 diabetes by varying periods of high fat diet in this strain of mouse (Parekh *et al.*, 1998; Muurling *et al.*, 2002; Huo *et al.*, 2003; Petro *et al.*, 2004). Though the diabetic manifestation in the present stock of mice is characterized by an impaired glucose intolerance at a higher basal glycemic status, certain degree of insulin sensitivity can be inferred from the recorded significantly higher glucose clearance on glucose challenge and, from the near identical glucose clearance in diabetic animals in comparison to non diabetic controls on insulin challenge. However, prevailing IR is clearly evidenced from the much higher glucose elevation rate seen in both GTT and IRT. Protective effect of OI extract is clearly evident from the significantly lower hyperglycemia and near normal GTT and IRT curves, and further, glucose elevation rates under both these tests are significantly lower in OI extract supplemented mice than in diabetic animals. These observations coupled with the noted minimal decrease in plasma insulin titre bespeak of both an insulinogenic action, as well as insulin sensitivity potentiating effect of OI extract. In recent times, herbal extracts and, compounds isolated from plants, have been shown to exert various effects on pancreas such as, β -cell proliferation, insulin synthesis and/or secretion suggesting the potential role of medicinal herbs in combating insulin resistance or insufficiency associated with diabetes, Whereas Huo *et al.* (2003) showed increased serum insulin levels on treatment with a mixture of eight herbal components, Muniappa *et al.* (2003) showed insulin secretagogue activity and cytoprotective role of *Scorparia dulcis* (Sweet Broomweed) and, Jayaprakasan *et al.* (2006) demonstrated the ability of anthocyanins and ursolic acid isolated from Cornelian cherry (*Cornus mas*) for enhanced islet function and elevated circulating serum insulin levels. Similarly, Leu *et al.* (2009) have also reported the competence of an extract of *Angelica hirsituflora* to serve as an insulin secretagogue. The OI extract

in our present study also seems capable of acting as an insulin secretagogues, as seen by the recovery of serum insulin level in OI supplemented group compared to diabetic animals.

In the conundrum of metabolic alterations associated with diabetes, changes in the activity levels of hepatic glucose metabolizing enzymes contribute substantially to hyperglycemia and insulin resistance. High fat diet induced type-2 diabetes in C57BL/6J mouse model, simulating human non-insulin dependent diabetes mellitus (NIDDM), has revealed lower level of glucokinase and higher levels of G-6-Pase and PEPCK mRNA. Glycogen being the principal storage form of glucose in liver and muscle regulated by insulin, diabetic insufficiency of insulin is likely to affect these glycogen stores by way of altered glucose transport and activity of glycogenic, glycolytic and gluconeogenic enzymes. In this context, tissue glycogen contents have been noted to be significantly lowered in diabetic mice, a change resisted to a greater extent by simultaneous feeding with OI extract. The decreased hepatic glucokinase mRNA expression together with increased G-6-Pase and PEPCK transcripts suggests decreased glucose entry and, increased glucose efflux and gluconeogenesis. Treatment with OI extract simultaneous to high fat diet, protected the levels of expression of these mRNAs in hepatic tissue to a significant effect denoting the ability of the extract to resist diabetogenic alterations. Some herbal preparations like *Trigonella foenum graecum* (Fenugreek) seed powder (Siddiqui *et al.*, 2006) and flavonoid rich extract from seeds of *Eugenia jambolina* (Sharma *et al.*, 2008) have been shown to reverse the effects on glucose transport and metabolizing enzymes in alloxan and streptozotocin induced diabetic rats and mice respectively. Taken with the previously noted effect on serum insulin level, the current protective effects seen on

glucose metabolizing enzymes suggest the potential of OI extract to act at the levels of both insulin production as well as insulin action.



Overall, the present study effectively shows that diet induced type 2 diabetes is characterized by hypoinsulinemia, decreased hepatic glucose uptake and glycogenesis, coupled with gluconeogenesis while, OI extract is adequately competent to counteract the effects of diet induced diabetic hyperglycemia and metabolic alterations. Our previous studies have recorded dose dependent hypoglycemic and hypolipidemic effects of OI extract in streptozotocin induced diabetic rats (Ansarullah *et al.*, 2009). Moreover, our preliminary assay of phytoconstituents present in OI extract has, revealed the presence of sterols, saponins, terpenoids, flavonoid glycosides and sugars (unpublished). Having demonstrated the potent effect of OI extract in combating type 2 diabetes induced glycemic dysregulation and alterations in carbohydrate metabolism, our further focus is on isolation of principles/compounds from the extract to test the bioactive molecule(s) for development as an alternative therapeutic agent against type-2 diabetes.

Influence of *Oreocnide integrifolia* extract on IRS-1, Akt and Glut-4 in high fat diet induced type-2 C57BL/6J mice

Introduction:

There were about 171 million diabetics worldwide at the turn of the century and the number is estimated to rise to 366 million by 2030 (Wild *et al.*, 2004). India has recorded the greatest increase in recent times and, with a current prevalence of 2.4% in the rural population and 11.6% in the urban population, it is estimated that by 2025 India will have the maximum number of diabetic subjects (King *et al.*, 1998; Tripathi and Srivastava, 2006). Though many drugs are commercially available for treating the disease, most of them are out of reach for many and are also beset with some adverse effects (Sharma *et al.*, 2008). Treatments are essentially aimed at controlling hyperglycemia, which includes insulin secretagogues (Sulphonylureas, meglitinides, GLP analogues) and insulin sensitizers which reduced hepatic glucose generation (Metformin) or enhance peripheral glucose uptake by muscle and adipose tissue (Metformin, thiazolidinediones) but, no drug in vogue intrinsically exerts both the effects (Tousch *et al.*, 2008). There is ethnic genetic variability on a global scale and indigenous medicinal plants are likely to be more effective on an adaptive evolutionary diversity. India is a country with a traditional history and heritage for herbal medicines (Grover *et al.*, 2002). The use of medicinal herbs in this context is a meaningful alternative and in recognition this fact; WHO has adverted research in this direction and affirmed that, traditional plant based treatments for diabetes warrant further attention (WHO, 1980). North eastern states of India support a rich

biodiversity (biodiversity hotspots) spanning from tropical rainforests to alpine scrubs with geographical and climatic diversity and hold approximately 50 percent of total flora of India. This region is the homeland for more than 150 ethnic groups (tribal or tribal in origin) and about 90 percent of the total population of the region has a rural background and most still live in remote, isolated areas, maintaining individual identities and a primitive economic life. In such a scenario, knowledge of medicinal plants remains poorly documented in scientific literature. These plants have found a prime place in the indigenous system of medicine and evaluation of their active ingredients is the need of the day. *Oreocnide integrifolia* (Gaud.) Miq (family Urticaceae) are trees of 5-20 m height having reddish brown branchlets and simple, alternate, spiral and clustered leaves at twig end, found in wet evergreen forests at 300-1400 m height. They are mainly distributed in India, China, Bhutan, Indonesia, Laos, Myanmar, Sikkim and Thailand (Chen *et al.*, 2003). The roots of *Oreocnide integrifolia* are mixed with ginger powder and applied for treatment of rashes by Khasi and Jaintia tribes of Meghalaya (Begum and Nath, 2000; Kharkongor and Joseph, 1981). In north eastern states of India it is popularly known as ukhajang (manipuri), bonrhea (assamese), gingsining (garo) and dieng teingbah (khasi), and an infusion prepared from the leaves is used as a decoction to alleviate diabetic symptoms. Type 2 diabetes mellitus is a metabolic disease with a plethora of heterogeneous interrelated manifestations and complications like hyperglycemia, hyperinsulinemia, insulin resistance, impaired glucose tolerance and peripheral utilization, decreased hepatic glycolysis, increased gluconeogenesis, dyslipidemia etc, all of which are related primarily to insulin and its action. Chronic hyperglycemia caused due to abnormalities in glucose metabolism and insulin resistance characterizes type 2 diabetes (McGarry, 1994). Liver being the prime centre of

glucose homeostasis, accumulation of hepatic lipids could contribute to insulin resistance (Kim *et al.*, 2000). Increased hepatic free fatty acid production and elevated plasma levels are characteristic of diabetic subjects. The higher serum free fatty acids levels lower the ability of insulin to suppress hepatic glucose production by activating gluconeogenesis and inhibiting glycolysis (Shah *et al.*, 2003; Kishore *et al.*, 2006). All these metabolic alterations associated with type 2 diabetes result from a relative insufficiency of insulin to overcome peripheral insulin resistance. A set of health problems like hyperlipidemia, atherosclerosis and hypertension linked to impaired carbohydrate and lipid metabolisms are all consequences of both insulin deficiency and resistance (Brosche, 2001; Jayaprakasam *et al.*, 2006). Any antidiabetic agent should exert ameliorative effect on the diabetic manifestations by enhancing insulin secretion and/or by improving /mimicking insulin action. Despite the existing treatment modalities, there is need for new treatment paradigms for type 2 diabetes to control the progressive metabolic deterioration (Turner *et al.*, 2005). Alternative agents being explored should be able to hit at the sites of basic defects alluded to the disease, which are essentially islet dysfunction in association with insulin resistance. Molecular mechanisms underlying these basic defects also need to be evaluated to have a better understanding. To facilitate such evaluations, appropriate clinically relevant experimental model is required. The C57BL/6J mice when fed with high fat diet develops all classical type 2 diabetic symptoms like insulin resistance and insufficient islet compensation, and hence serves as an ideal model for studying pathophysiology of impaired glucose tolerance and type 2 diabetic manifestations at molecular level (Ahren *et al.*, 1997; Ahren and Pacini, 2002; Winzell *et al.*, 2003; Prpic *et al.*, 2003; Reimer *et al.*, 2002). This mouse also serves as a good model for evaluating the efficacy of new antidiabetic agents as well. (Ahren *et al.*, 1999; Ahren

et al., 2000a; Ahren *et al.*, 2000b). Natural products from medicinal plants are of focal interest in the discovery of new chemical entities in modern drug discovery programs. To take the program to such finer points, there is need to evaluate the efficacy of a wide variety of botanicals that are part of folklore medicine. It is in this context that we had initiated studies on *Oreocnide integrifolia* (Gaud.) Miq (OI) used by people in north eastern part of India. Previously, we had demonstrated potent antihyperglycemic and antihyperlipidemic effects of OI leaf extract in streptozotocin induced diabetic rats (Ansarullah *et al.*, 2009). Thus, the present study was planned to evaluate whether (i) the OI extract brings about insulin secretion in vivo and in vitro and (ii) whether it is mediated through the insulin-signaling pathway.

Materials & Methods:

Plant extract preparation: As given in Chapter 1.

Animals and Diets: Male C57BL/6J mice (age 4-5 weeks) were purchased from National Centre for Laboratory Animal Service, National Institute of Nutrition, Hyderabad, India. To make a fully developed insulin resistant DIO (diet induced obese) animal phenotype, 20 animals were fed with high-fat diet (60 kcal% fat, D12492 Research Diet, New Brunswick, NJ); 20 with high fat diet supplemented (mixed with feed) with 3% O.I extract and 20 on standard laboratory diet for 3 months. BALB/c mice (age 5-6 months) were used for islet culture and insulin secretion assays. The experiment was carried out according to the guidelines of the Committee for the Purpose of Control and Supervision of Experiments on Animals, India and approved by the Animal Ethical Committee of Department of Zoology, The M.S University of Baroda, Vadodara (Approval No. 827/ac/04/ CPCSEA)

Metabolic parameters: As given in Chapter 3c.

Plasma Glucose and Insulin: As given in Chapter 3a.

Protein Expression Analysis:

Sample Preparation: Plasma membrane and cytosolic fractions from triceps muscle of control and experimental animals were prepared as described by Drombowski *et al.* (1996) and Kristiansen *et al.* (2001).

Reagents

- **Protease inhibitor:** Commercially available protease inhibitor cocktail (Sigma Chemical Company, USA.) was used.
- **Phosphatase inhibitor:** 47mg Trisodium phosphate (Na_3PO_4), 42mg Sodium fluoride (NaF), 4mg Sodium orthovanadate (Na_3VO_4), and 635mg β -glycerophosphate were dissolved in 10ml with homogenization buffer.
- **Buffer – A (pH7.0):** 84 mg of sodium bicarbonate (NaHCO_3) was dissolved in 75ml of distilled water and pH adjusted to 7. To this, 8.5575g sucrose, 1.742mg phenylmethylsulfonylfluoride (PMSF) and 32.5mg sodium azide (NaN_3), protease (10 $\mu\text{l/ml}$) and phosphatase inhibitors (100 $\mu\text{l/ml}$) were added and made up to 100ml with distilled water.
- **Buffer – B (pH7.0):** 84mg of sodium bicarbonate (NaHCO_3) was dissolved in 75ml of distilled water and pH adjusted to 7. To this, 1.742mg PMSF, 32.5mg sodium azide and protease inhibitor were added and made up to 100ml with distilled water.

- **Sucrose gradient (w/w):** A discontinuous sucrose density gradient prepared by layering successive decreasing sucrose density solution upon one another. The preparation and centrifugation of a discontinuous gradient containing sucrose solution from 25, 32 and 35%. This gradient gives good separation of plasma membrane fraction.
- **25% sucrose (w/w):** For 20ml of 25% sucrose, 5g of sucrose was dissolved in 15g of buffer B.
- **32% sucrose (w/w):** For 20ml of 32% sucrose, 6.4g of sucrose was dissolved in 13.6g of buffer B.
- **35% sucrose (w/w):** For 20ml of 35% sucrose, 7g of sucrose was dissolved in 13g of buffer B.

Preparation of sucrose gradient

The gradient was prepared by layering progressively less dense sucrose solution upon one another. Briefly, sucrose solutions were added into the polyallomer tube (Ultracentrifugation tube) slowly and steadily, starting with the 35% solution. First 2ml of the 35% solution had drained into the tube, and then 2ml of 32% solution could be loaded on top of the 35% solution. This procedure was continued with 1ml of 25% solution. There was enough space left at the top of the tube upon which to load the 0.5ml of sample.

Subcellular fractionations

Triceps muscle tissue from control and experimental animals were simultaneously processed for preparation of different fractions. All steps were carried out on ice or at 4°C. Tissue (~1 g) was first cleaned of all visible fat, nerve, and blood

vessels and minced in buffer – A. The minced tissue was homogenized (1 g/ 1.5 ml of buffer-A) using a polytron equipped homogenizer at a precise low setting. The resulting homogenate was centrifuged at 1,300xg for 10 min. The supernatant was centrifuged at 1, 90,000xg for 1 h. The resultant supernatant was saved, and sampled as a cytosolic fraction for IR, GLUT4, Akt and phospho Akt protein analysis. The pellet was resuspended in buffer-A, and applied on discontinuous sucrose gradients (25%, 32% and 35% w/w) and centrifuged at 1,50,000xg for 16 h. Plasma membrane at 25–32 interfaces were recovered, diluted with buffer-B, and centrifuged at 1,90,000xg for 1 h. Plasma membrane fraction (pellet) was resuspended in buffer-A and kept at –80°C until used for GLUT4 and IR protein expression analysis. Protein concentration in the sample was determined prior to the western blot analysis.

Estimation of protein

Protein concentration was determined as per the method of Lowry *et al.* (1951) with bovine serum albumin (BSA) as the standard (as given in chapter 1).

Western blot analysis: Separation of proteins

Proteins were separated by SDS - Polyacrylamide gel electrophoresis as described by Laemmli ,(1970).

Principle

SDS – PAGE involves the separation of proteins based on their size. By heating the sample under denaturing and reducing conditions, proteins become unfolded and coated with SDS detergent molecule, acquiring a high net negative charge that is proportional to the length of the polypeptide chain. When loaded on to a gel matrix and placed in an electric field, the negatively charged protein molecules

migrate towards the positively charged electrode and are separated by a molecular sieving effect. Molecular weight protein marker that produces bands of known size is used to help identify proteins of interest.

Reagents

- **Acrylamide/Bis (30% T, 2.67% C):** 29.2g acrylamide and 800g N'N'-bis-methylene-acrylamide were dissolved in 100ml of deionized water. Filtered and stored at 4°C in the dark (30 days maximum).
- **10% (w/v) SDS:** 10g SDS was dissolved in 90ml water with gentle stirring and brought to 100ml with deionized water.
- **1.5 M Tris – HCl (pH 8.8):** 18.15g Tris base was dissolved in 80ml deionized water. Adjusted to pH 8.8 with 6N HCl and brought total volume to 100ml with deionized water and stored at 4°C.
- **0.5 M Tris – HCl (pH 6.8):** 6g Tris base was dissolved in 60ml deionized water. Adjusted to pH 6.8 with 6N HCl and brought the total volume to 100ml with deionized water and stored at 4°C.
- **10% APS (Fresh daily):** 100mg ammonium persulfate was dissolved in 1ml of deionized water.
- **N' N' - Tetramethyl ethylene diamine (TEMED) :** Commercially available.
- **Sample buffer (SDS Reducing buffer) (pH 6.8):** 1.25ml 0.5M Tris-HCl (pH 6.8), 2.5ml glycerol, 2ml 10% (w/v) SDS were added to 0.2ml of 0.5% (w/v) bromophenol blue and brought total volume to 9.5ml with 3.55ml

deionized water. Stored at room temperature. 50 μ l β -mercaptoethanol was added to 950 μ l of sample buffer prior to use.

- **10X electrophoresis buffer (pH 8.3):** 30.3g Tris base, 144.0g Glycine and 10g SDS were dissolved in 800ml deionized water and brought total volume to 1 litre with deionized water and stored at 4°C.

Procedure

Preparation of Gel (10ml)

10 % running gel was prepared by mixing the reagents as shown below.

Deionized H ₂ O	– 4.1ml
30% degased acrylamide/bis	– 3.3ml
1.5 M Tris – HCl (pH 8.8)	– 2.5ml
10 % (w/v) SDS	– 0.1ml

7 % running gel was prepared by mixing the reagents as shown below.

Deionized H ₂ O	– 5.1ml
30% degased acrylamide/bis	– 2.3ml
1.5 M Tris – HCl (pH 8.8)	– 2.5ml
10 % (w/v) SDS	– 0.1ml

Gently mixed and degassed the mixture for 15 minutes. 50 μ l of 10% APS and 5 μ l TEMED were added prior to pouring the gel and swirled gently to initiate polymerization. This mixture was poured into 1mm thickness gel casting plate setup and allowed to 20–30 minutes for polymerization.

5 % stacking gel was prepared by mixing the reagents as given below.

Deionized H ₂ O	– 5.7ml
30% degased acrylamide/bis	– 1.7ml
0.5 M Tris – HCl (pH 6.8)	– 2.5ml
10 % (w/v) SDS	– 0.1ml

Gently mixed and degassed the mixture for 15 minutes. 50 μ l of 10% APS and 10 μ l TEMED were added prior to pouring the gel and swirled gently to initiate polymerization. This mixture was added on top of the 10% running gel. Then, the comb (1mm thickness) was inserted and allowed to form the well.

Loading of proteins

Equal volume (25 μ g) of samples from triceps muscle of control and experimental animals were diluted with sample buffer (1:2), heated at 95°C for 4 minutes and then cooled on ice for 5 minutes. Samples were loaded to 10% and 7% SDS–PAGE in a Bio–Rad miniature slab gel apparatus. The prestained broad range protein molecular weight markers used were myosin (198kDa), β -galactosidase (116kDa), bovine serum albumin (85kDa), ovalbumin (54kDa), carbonic anhydrase (37kDa), soybean trypsin inhibitor (29kDa), lysozyme (19kDa) and aprotinin (6kDa) (Bio-Rad). Electrophoresis of protein was performed at 100V (constant) until the dye front reaches the bottom of the running gel.

Transfer of proteins to the membrane and immunoblotting

Reagents

- **Transfer buffer**

3g Tris and 25g glycine were dissolved in 800ml of double distilled water and made up to 1000ml with 200ml of methanol.

- **Polyvinylidene difluoride (PVDF) membrane (Amersham Biosciences Ltd., UK)**
- **TBS (Transfer Buffer Saline)**

4g of NaCl and 10ml of 1M Tris HCl (pH 7.6) were dissolved in 450ml of distilled water, adjusted the pH to 7.6 and made up to 500ml with distilled water.

- **TBS-T:** 500µl of Tween-20 was dissolved in 500ml of TBS and the pH was adjusted to 7.6.
- **5% Blocking solution**

500mg of blocking reagent was dissolved in 10ml of TBS-T solution.

Primary antibodies:

IRS (Insulin Receptor Substrate 1): Insulin receptor substrate 1 (IRS-1) is one of the major substrates of the insulin receptor kinase (1). IRS-1 contains multiple tyrosine phosphorylation motifs that serve as docking sites for SH2 domain containing proteins that mediate the metabolic and growth promoting functions of insulin. IRS-1 also contains over 30 potential serine/ threonine phosphorylation sites

Glucose transporter subtype-4 (GLUT4): GLUT4 (H-61) Rabbit mAb detects endogenous levels of total GLUT4 of rat, human and mouse. Polyclonal antibodies are produced by immunizing rabbits with amino acids 230-290 cytoplasmic GLUT4 of human origin.

Akt: Akt (H-136) Antibody detects endogenous levels of total Akt of rat, human and mouse. Polyclonal antibodies are produced by immunizing rabbits with amino acids 345-480 of Akt1/2 of human origin.

Procedure

After the separation of proteins by SDS-PAGE, the stacking gel was cut and discarded; the separating gel was briefly rinsed in distilled water 2-3 min and then equilibrated in cold transfer buffer under gentle agitation for 5-10 min. In the mean time, fiber pad and Whatman paper and PVDF membrane were soaked in cold transfer buffer. Transfer sandwich was assembled in the following order from anode (+) to cathode (-).

- a) + ve end
- b) Fiber pad
- c) Filter paper soaked in transfer buffer
- d) PVDF Membrane
- e) Gel
- f) Filter paper soaked in transfer buffer
- g) Fiber pad
- h) -ve

The setup was placed in the transfer apparatus filled with cold transfer buffer and subjected to an electric current at 100V for 1h under cold condition. After the transfer, the PVDF blot was removed from the transfer system blocked the unreacted sites on the membrane to reduce the amount of non-specific binding during subsequent steps in the assay using 5% blocking solution for 1h. After the blocking is over, decanted the blocking solution and rinsed the membrane in TBS-T After the blocking is over, decanted the blocking solution and rinsed the membrane in TBS-T and incubated for 1h in anti-GLUT-4 (1:2000; generous gift from Dr Samuel Cushman, NIDDK, USA), anti-IRS-1 (1:1000; Cell Signaling, USA), Akt-1 (1:1000;

Cell Signaling, USA) and β -actin (1:2000; Santa Cruz Biotechnology, USA) primary antibodies at room temperature, which were diluted in TBS-T. Following incubation, the blot was washed for three times (5 minutes each) with TBS-T. After washing, the blot was incubated for 1h with horseradish peroxidase conjugated rabbit secondary antibody, which was diluted 1:5000 with TBS-T. Following incubation, the blot was washed for three times (5 minutes each) with TBS-T. Drained the excess wash buffer from the washed blot and placed them, protein side up on a sheet of Saran Wrap™. The detection reagent mixture [an equal volume of detection solution 1 with detection solution 2 (Enhanced Chemiluminescence, Amersham Biosciences, UK.)] was pipetted on to the blot and incubated for 30-60 seconds and drained off excess reagent. The blotted protein was quantified using Quantity one software system (Bio-Rad Laboratories, CA).

Stripping and reprobing the membrane

Membrane was stored wet wrapped in Saran Wrap™ in a refrigerator (2-8 °C) after immunodetection. The membrane was submerged in stripping buffer [62.5mM Tris-HCl (pH 6.7); 2% SDS; 100mM 2-mercaptoethanol] and incubated at 50 °C for 30 minutes with occasional agitation. Then the membrane was washed for 2 times (each 10 minutes) in TBS-T at room temperature using large volume of wash buffer. The membrane was blocked by immersing in 5% blocking solution for 1 h at room temperature. After the blocking is over, decanted the blocking solution and rinsed the membrane in TBS-T and incubated for 1h in β -actin antibody at room temperature, which was diluted 1:5000 with TBS-T. The immunodetection protocol was repeated as detailed previously.

Immunostaining and Confocal Microscopy: The pancreas were aseptically removed from respective treatment groups and fixed in 4% fresh paraformaldehyde. The tissues were subsequently embedded in paraffin wax and sectioned at 5µm thickness with a microtome (Leica, Wetzlar, Germany) and mounted on poly-L lysine (Sigma, MO) coated slides. Slides were deparaffinised, downgraded in xylene, alcohol and blocked with 4% normal donkey serum and then incubated with antisera. Guinea pig anti-insulin antibody (Linco Research Inc, St. Charles, MO), mouse antiglucagon (Sigma, St. Louis, MO), were used at 1:100 dilutions. Alexa-Fluor 488 and Alexa-Fluor 546 F(ab')₂ secondary antibodies (Molecular Probes, OR) were used at 1:200 dilution. Hoechst 33342 was used to visualize nuclei. Primary antibodies were incubated overnight at 4°C, washed with calcium-magnesium containing PBS and then incubated with the secondary antibodies at 37°C for 1 hour. Slides were washed extensively in PBS and mounted in Vectasheild (Vectorlabs). Confocal images were captured using a Zeiss LSM 510 laser scanning microscope using a 63×/1.3 oil objective with optical slices ~0.8 µm. Magnification, laser and detector gains were set below saturation and were identical across samples.

Statistical analysis: Statistical evaluation of the data was done by one way ANOVA followed by Bonferroni's Multiple comparison test .The results are expressed as mean ± S.E. or ± S.D Mean using Graph Pad Prism version 3.0 for Windows, Graph Pad Software, San Diego, California USA.

Result:

Metabolic parameters: As given in Chapter 3c

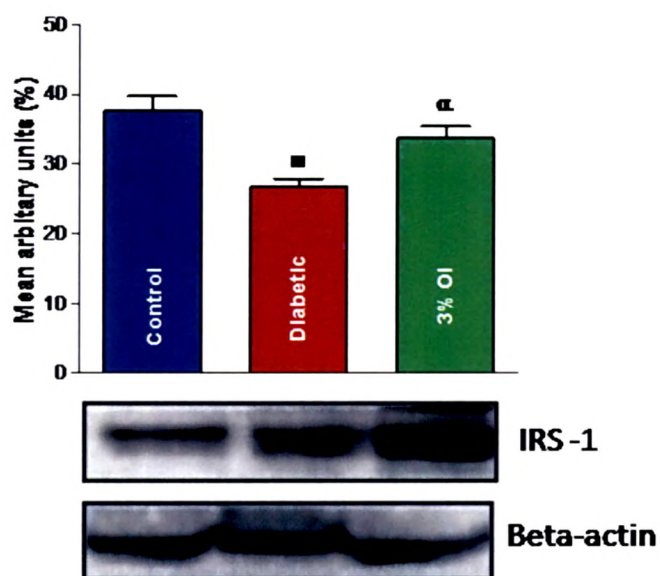
Plasma glucose levels and insulin titre: As given in Chapter 3a

Western blot analysis: Immunoblot analysis was carried out in control, diabetic and OI extract fed groups wherein protein expression pattern of molecules involved in insulin signaling pathway was evaluated in gastrocnemius muscle. IRS-1 expression in muscle (cytosolic fraction) was decreased significantly ($P < 0.001$) in diabetic mice compared to controls while OI extract supplemented animals depicted higher near normal level when compared to diabetic animals (Fig. 1). However, AKT-1 expression (cytosolic fraction) of control, diabetic or OI treated group did not show any significant difference (Fig. 2). Effect on Glut-4 distribution was evaluated in both cytosolic and plasma membrane fractions (Fig. 3 & Fig. 4). Cytosolic fraction showed no significant changes in Glut-4 protein expression in either control or experimental groups of animals. However, membrane glut-4 expression was remarkably reduced ($P < 0.0001$) in diabetic animals and there was a conspicuous maintenance of Glut-4 expression in OI supplemented group though yet lesser than in control animals.

Insulin/glucagon immunostaining of pancreas: (Fig. 5).

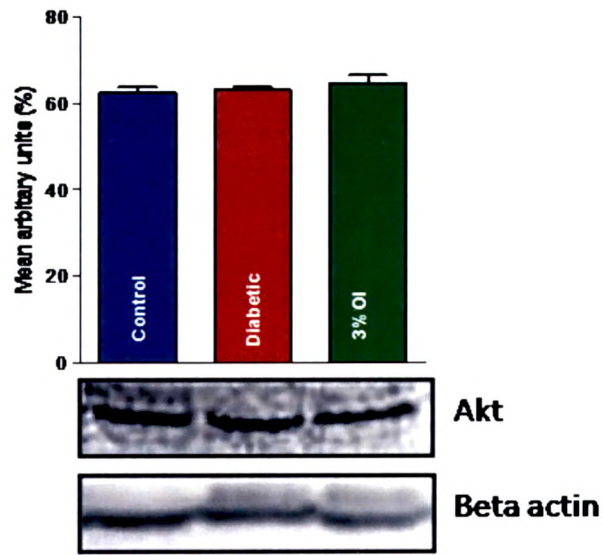
Diabetic mice showed weak staining for insulin while the OI extract-supplemented group showed remarkable insulin immunopositivity closest to the control islet response. However, there was no significant change in glucagon-positive cells in control and experimental groups.

Fig. 1. Immunoblot analysis of Insulin receptor substrate-1 expression in Red Gastrocnemius Muscles in control and experimental animals



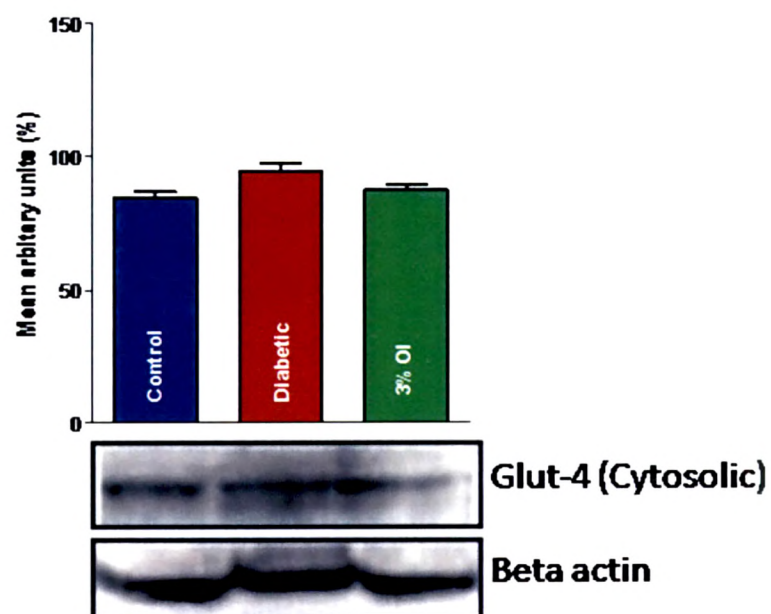
♦- $p < 0.01$, ■- $p < 0.001$, ◆- $p < 0.0001$: Experimental groups compared to control group
 α- $p < 0.01$, β- $p < 0.001$, δ- $p < 0.0001$: OI treated group compared to diabetic group

Fig. 2. Immunoblot analysis of Akt in Red Gastrocnemius Muscles of control and experimental animals



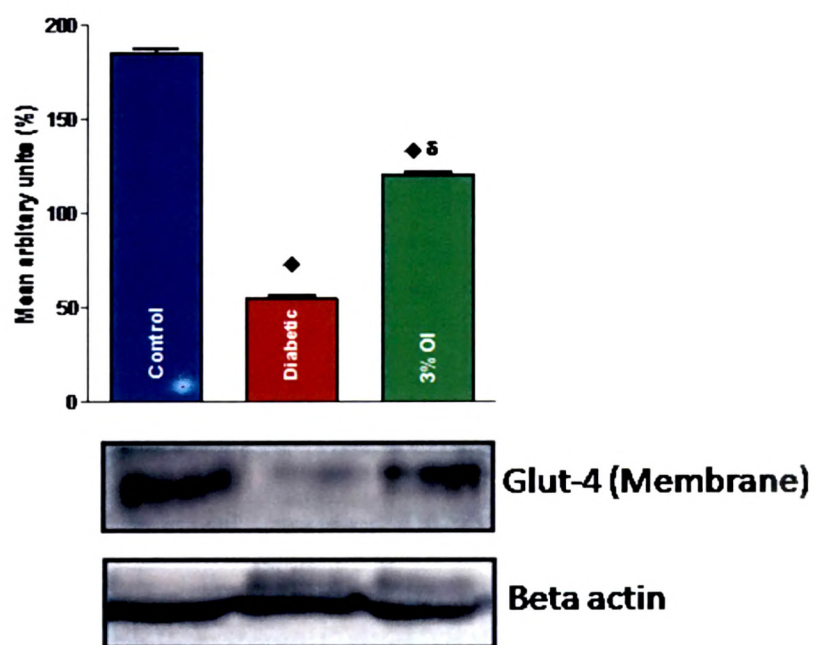
•=p<0.01, ■=p<0.001, ◆=p<0.0001: Experimental groups compared to control group
α=p<0.01, β=p<0.001, ⚡=p<0.0001: OI treated group compared to diabetic group

Fig. 3. Immunoblot analysis of Cytosolic GLUT-4 in Red Gastrocnemius Muscles in control and experimental animals



●=p<0.01, ■=p<0.001, ◆=p<0.0001: Experimental groups compared to control group
 α=p<0.01, β=p<0.001, ⚡=p<0.0001: OI treated group compared to diabetic group

Fig. 4. Immunoblot analysis of Membrane Glut-4 in Red Gastrocnemius Muscles in control and experimental animals



● $p < 0.01$, ■ $p < 0.001$, ◆ $p < 0.0001$: Experimental groups compared to control group
 α $p < 0.01$, β $p < 0.001$, δ $p < 0.0001$: OI treated group compared to diabetic group

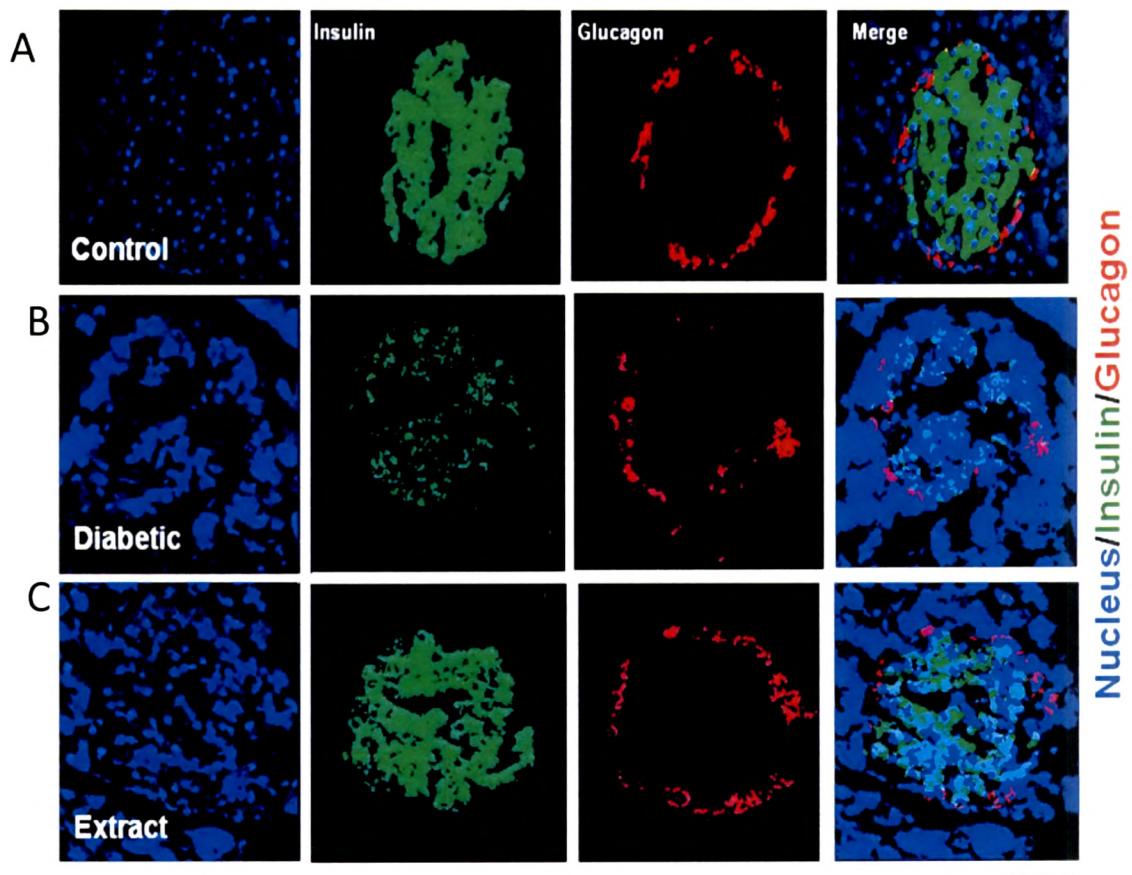


Fig 5 : Images represent immunostained section of pancreas of A) Control, B) Diabetic and C) Diabetic + OI 3%. Guinea Pig anti insulin (green) and mouse glucagon (red) were used as primary antibodies while alexaflour 488 and alexaflour 546 as $F(ab')_2$ secondaries. Hoechst 33342 (Blue) was used to visualize nuclei. The slides were visualized by Laser Scanning Confocal Microscope (LSM 510 META, ZEISS, Germany) using Argon and Krypton Lasers. Optical slices were taken at $\sim 0.8\mu\text{m}$. Laser gains, pin hole setting and magnification were set identical across samples. Scale bar represents $100\mu\text{m}$.

Discussion:-

The high-fat diet-fed C57BL/6J mouse is an ideal model for studying mechanisms of impaired glucose tolerance along with insulin resistance leading to type 2 diabetes marked by islet dysfunction and for developing novel therapeutic interventions (Winzell and Ahren, 2004). The study has tried to evaluate the influence of OI extract on insulin signaling pathway in the muscle of diabetic and non-diabetic C57BL/6J mouse. The C57BL/6J mouse developed type 2 diabetic manifestation when fed continuously for 24 weeks with a high-fat diet. Diabetic induction was marked by loss of insulin-positive cells in islets, >200% decrease in fasting plasma glucose and >20% decrease in plasma insulin level accompanied by decreased expressions of IRS-1 and membrane Glut-4 in the muscle. Supplementation with OI extract is able to ameliorate the diabetic manifestations marked by noticeable insulin immunoreactivity in the islets and improved plasma insulin titre and glycemic level suggesting, both an insulinogenic action as well as insulin sensitivity-potentiating effect of the OI extract. In recent times, herbal extracts and compounds isolated from plants have been shown to have various effects on pancreas, such as β -cell proliferation, insulin synthesis and secretion, suggesting the potential role of medicinal herbs in combating insulin resistance and insufficiency associated with diabetes; further, Huo et al. (2003) showed increased serum insulin levels on treatment with a powder mixture of eight herbal components. Qin et al. (2004) showed that Gosha-jinki-gan (a herbal complex) ameliorates abnormal insulin signaling. Similarly, Muniappa et al. (2004) showed insulin secretagogue activity and cytoprotective role of *Scorparia dulcis* (Sweet Broomweed) and Jayaprakasan et al. (2006) demonstrated the ability of anthocyanins and ursolic acid isolated from the Cornelian cherry (*Cornus mas*) for enhanced islet function and elevated circulating serum insulin

levels. Similarly, Leu et al. (2009) have also reported competence of an extract of *Angelica hirsutiflora* to serve as an insulin secretagogue. The OI extract in our present study seems capable of acting as a secretagogue as well, and this is confirmed by the in vitro ability of the extract to bring about insulin release from isolated BALB/c mice islets in a dose-dependent manner (Chapter 4). The current protective effects seen suggest potential of OI extract to act at the levels of both insulin production as well as insulin action. The principal action of insulin on glucoregulation is through peripheral tissue uptake and metabolism. Muscle and adipose tissue are the main insulin-sensitive tissues involved in this process. A defect in insulin receptor or post-receptor signalling mechanism can have profound effect in terms of insulin insensitivity. Number of molecular lesions in muscle and adipose tissue are known to exacerbate diabetic symptoms and can even be a major cause of type 2 diabetes (Sharma *et al.*, 2008). Western blot analysis of some proteins involved in insulin-induced glucose metabolism in the muscle tissue in the present study has revealed significantly decreased membrane Glut-4 and cytosolic IRS-1 expressions in high-fat diet-induced type 2 diabetes. However, Akt-1 was not significantly compromised. Apparently, high fat-diet-induced type 2 diabetes in C57BL/6J mice has defective peripheral glucose utilization due to deficiency in IRS-1, resulting in downstream defect in Akt-1–PI-3 kinase activation. This in turn leads to non-phosphorylation of Glut-4 and its membrane translocation contributing to reduced glucose transport (Tremblay *et al.*, 2001). Glut-4 is the insulin-sensitive glucose transporter in skeletal muscle and adipose tissue and its importance in whole body glucose metabolism has been elucidated using experimental models of Glut-4 null mice (Charron *et al.*, 2005). Recently, Liu et al. (2009) demonstrated the action of Dang Gui Bu Xue Tang (herbal formulation) on Glut-4 translocation in fructose-fed rats. Of late, attention has shifted

to herbal extracts/constituents as potential agents for treatment of type 2 diabetes. Identifying targets of action of herbal preparations is an essential aspect of therapeutic drug development in combating molecular lesions characteristic of insulin resistance and type 2 diabetes. There is, therefore, a need to evaluate the efficacy of herbal extracts/principles on a composite scale with regard to molecular defects in peripheral insulin resistance/glucose utilization. Although there are a few studies on plant products/principles on this aspect, their obvious drawbacks lie in the fact that these studies are either on cultured myoblast cells or on alloxan/streptozotocin-induced type 1 diabetic animals and that too restricted to only Glut-4 concentration or glucose uptake (Balakrishnan *et al.*, 2005; Siddqui *et al.*, 2006; Daisy and Jasmine, 2008; Cazarolli *et al.*, 2009; Gireesh *et al.*, 2009). The present study, in this context, has tried to assess cytosolic and membrane Glut-4, Akt-1 and IRS-1 expressions. The study clearly shows that OI extract is able to prevent, high-fat diet-induced type-2 diabetic manifestations of under-expression of IRS-1 protein and hampered membrane translocation of Glut-4 transporter in the skeletal muscle (Fig. 3, 3a and Fig 4, 4a). Overall, the present study effectively shows that diet-induced type 2 diabetes is characterized by significant islet dysfunction (β -cell loss), with consequent hypoinsulinemia and peripheral deficiency in glucose uptake by insulin-sensitive peripheral tissues (muscle) and that, OI extract is adequately competent to counteract these effects of diet-induced diabetic manifestation.

The influence of *Oreocnide integrifolia* (Gaud.) miq extract on type 2 diabetes induced dyslipidemia, leptin titres and intra-islet leptin localization on high fat fed *C57BL/6J* mice.

Introduction:-

Whereas changes in lipid metabolism are a consequence of type 1 diabetes, there is both a cause and consequence relationship between lipid metabolism and type 2 diabetes. More than 16 million people are known to be afflicted by type 2 diabetes, the world over. Though there is a strong involvement of genetic component, it is also linked with obesity, a previous history of maturity onset diabetes and progressive development. The early stages of onset of type 2 diabetes are marked by tissue unresponsiveness to insulin, hyperglycemia, hyperinsulinemia and a more or less normal looking glucose tolerance curve with a blunted first phase insulin release. Along with a higher fasting plasma glucose (> 100 mg/dl and < 120 md/dl) the oral glucose tolerance test (OGTT) reveals basal and stimulated hyperinsulinemia and deterioration in the ability to handle glucose. Progression of the condition results in further increase in fasting blood glucose (> 126 mg/dl) which remains higher even by 2 hours during an OGTT and the hyperinsulinemic status fails to compensate for insulin resistance. Due to this inability of insulin to rein in the prevailing hyperglycaemia, it is also christened as non-insulin dependent diabetes (NIDDM). Ectopic deposition of lipids contributes to the etiology and progression of NIDDM forming the basis of lipotoxicity hypothesis.

Bad places for excess lipid deposition are the liver, skeletal muscle, pancreas and heart muscle. Persistent imbalance between energy intake and expenditure results in increased adipose mass and physical obesity (Surwit *et al.*, 1988; Stunkard, 1996; Weiser *et al.*, 1997). Obesity *per se* is in itself a high risk factor for type 2 diabetes and insulin resistance (Hartz *et al.*, 1983). Diabetes associated obesity is mainly central with overloaded abdominal fat deposits. Due to restraint anti-lipolytic action of insulin type 2 diabetes, portal circulation is flushed with free fatty acids thereby exposing non-adipose tissues to excess fat. This essentially leads to ectopic triglyceride accumulation in the above mentioned organs contributing to insulin resistance (Kim *et al.*, 2000) and β -cell dysfunction. Higher energy intake as against poor energy dissipation is a feature of modern life style and dietary habits. Fast food and soft drink syndrome especially in younger generation and even in older ones is fanning the fire of type 2 diabetes and metabolic syndrome. The combination of soft drink and fast food together contribute to both hyperglycemia and hyperlipidemia. The higher level of circulating free fatty acids and insulin resistance promote elevated hepatic glucose production through gluconeogenesis and inhibition of glycolysis (Hawkins *et al.*, 2003; Shah *et al.*, 2003).

Type 2 diabetes is the principal causative factor for death due to coronary artery disease. The hallmark symptoms of hyperglycemia, formation of advanced glycation end products, increased oxidative stress, hypertriglyceridemia, high LDL:HDL ratio, hyperinsulinemia, hypertension and genetic predispositions are all factors that can accelerate diabetic atherosclerosis. The ever-increasing incidence of diabetes with the global spread of central obesity has led to an estimate of three to four fold increases in cardiovascular disorders resulting in mortality (Nicholls *et al.*, 2010; Subramaniam and Rao, 2010).

Increased adiposity is related with the secretion of leptin, an adipocytic hormone, whose serum level is known to be proportional to body fat mass (Zang *et al.*, 1994; Haffer *et al.*, 1995; Bornstein *et al.*, 2000). Leptin has a major role in the critical control of body weight by suppression of food intake through satiety centre and promotion of energy expenditure (Halaas *et al.*, 1995; Friedman and Halaas, 1988; Ahima and Flier, 2000; Myers, 2004; Margetie *et al.*, 2002; Niswender and Schwartz, 2003; Sandoval and Davis, 2003; Sahu, 2004) besides other functions like reproduction, immunity etc (Flier, 1997; Lord *et al.*, 1998; Howard *et al.*, 1999; Duggal *et al.*, 2000). Many studies on rodents deficient in leptin or leptin signalling, leptin administration to ob/ob mice, favourable influence of leptin in ob/ob diabetic mice and pair feeding of ob/ob mice, all tend to suggest a role for leptin in glucose homeostasis independent of the effects on food intake and body mass (see Covey *et al.*, 2006). Such a role of leptin is deduced by studies on acute intracerebroventricular administration of leptin (Kamohara *et al.*, 1997). Apart from centrally mediated action of leptin on hypothalamus in promoting glucose uptake in muscle, adipose tissue and heart through a β -adrenergic mechanism (Haque *et al.*, 1999), a direct action of the hormone on the insulin sensitive tissues like liver, muscle and heart through leptin receptors is also demonstrated (Ghilardi *et al.*, 1996). Interestingly, leptin injection has also been shown to reverse hyperinsulinemia and augment tissue glucose utilisation by a synergistic action of central leptin and peripheral insulin (Haque *et al.*, 1999). There are also reports suggesting a modulatory action of leptin on insulin mediation (Cohen *et al.*, 1996; Muoio *et al.*, 1997; Seigrist-Kaiser *et al.*, 1997). It has also been shown by Huan *et al.* (2003) that, attenuated leptin receptor expression in adipose tissue can result in hyperinsulinemia and glucose intolerance, though, genetic deficiency of leptin receptors in liver is without any effect on plasma glucose or

insulin levels (Cohen *et al.*, 2001). All these go to prove that, serum leptin levels are co-relatable with body mass index, serum insulin level and insulin resistance. Moreover, the recent reports of leptin expression in pancreatic islets (Vickers *et al.*, 2001) and suggestion of insulin producing β -cells as a target of leptin action constituting a potential mechanism of regulation of glucose homeostasis (Ghilardi *et al.*, 1996; Kieffer *et al.*, 1996; Emilsson *et al.*, 1997; Seufert *et al.*, 1999b) together with the demonstration of leptin induced suppression of insulin synthesis and release in vitro (Emilsson *et al.*, 1997; Kieffer *et al.*, 1997; Kulkarni *et al.*, 1997; Okuno *et al.*, 1998; Seufert *et al.*, 1999a, b) make the story of leptin- insulin interactions, obesity and diabetes a heady concoction deserving more scathing scientific scrutiny.

It is in this background that, serum lipid profile together with insulin and leptin levels and immunolocalization of leptin in pancreatic islets and PPAR- γ mRNA expression in adipocytes have been undertaken in high fat diet induced type 2 diabetic BL 6 mice.

Materials and Methods:

Metabolic parameters: Body weight and food intake were recorded during the study period. At the end of the specified 24 weeks, animals were sacrificed, photographed for morphology of visceral adipose while muscle and pancreas were extracted for evaluation of other parameters. Hematoxylin–eosin staining was performed in paraffin sections for histological analysis of adipose tissue.

Plasma lipid profile: As mentioned in Chapter 1

Plasma leptin measurements: Plasma Leptin levels were determined using mouse leptin ELISA kit (Alexis Biochemicals, San Diego, CA). Principle: Briefly, standards, quality controls and samples are incubated in microtitration wells coated with anti-mouse leptin antibody. After a thorough wash, biotin labeled polyclonal antimouse leptin antibody is added to the wells and incubated with the immobilized antibody-leptin complex. After one hour incubation and a next washing step, streptavidin-horseradish peroxidase conjugate is added and incubated for half an hour. After last washing step, the conjugate bound is allowed to react with the substrate (H_2O_2 -tetramethylbenzidine). The reaction is stopped by addition of acidic solution, and absorbance of the resulting yellow product is measured spectrophotometrically at 450 nm. The absorbance is proportional to the concentration of leptin. A standard curve is constructed by plotting absorbance values versus leptin concentrations of standards, and concentrations of unknown samples are determined using this standard curve.

Preparation of samples: Dilute mouse serum 20 fold with Dilution Buffer.

If expected concentrations of leptin are very low, dilute samples only 1:10 with Dilution Buffer.

Assay procedure

1. Pipet 100 μ l of Standards, Quality control and diluted samples, preferable in duplicates, into the appropriate wells.
2. Incubate the plate at room temperature (ca. 25°C) for 1 hour, shaking at ca. 300rpm on an orbital microplate shaker.
3. Wash the wells 3-times with Wash Solution (350 μ l per well)

4. Add 100 μ l of the diluted Biotin Labeled Anti-mouse Leptin Antibody Solution into each well.
5. Incubate the plate at room temperature (ca. 25°C) for 1 hour, shaking at ca. 300 rpm on an orbital microplate shaker.
6. Wash the wells 3-times with Wash Solution (350 μ l per well).
7. Add 100 μ l of Streptavidin-HRP Conjugate solution.
8. Incubated the plate at room temperature (ca. 25°C) for 30 minutes, shaking at ca. 300 rpm on an orbital microplate shaker.
9. Wash the wells 3-times with Wash Solution (350 μ l per well)
10. Add 100 μ l of Substrate Solution (Avoid exposing the microtiter plate to direct sunlight. Covering the plate with e.g. aluminum foil)
11. Incubate the plate for 10 minutes at room temperature. (The incubation time may be extended [up to 20 minutes] if the reaction temperature is below 20°C.)
12. Stop the colour development by adding 100 μ l of Stop Solution.
13. Determine the absorbance by reading the plate at 450 nm. (optionally, to measure in dual wavelength mode 620-650 nm filter can be used to measure the reference absorbance. The absorbance should be read within 5 minutes following step 12.)

Note: if the microplate reader is not capable of reading absorbance greater than the absorbance greater than the absorbance of the highest standard, perform a second reading at 405 nm. Anew standard curve, constructed using the values measured at 405 nm, is used to determine leptin concentration of off-scale samples. The readings at 405 nm should not replace the on-scale readings at 450 nm.

Calculations

The calibration curve was constructed by plotting the absorbance (Y) of standards versus *log* of the known concentration (X) of standards. Results are expressed as concentration of leptin (pg/ml) in samples.

Leptin Immunofluorescence: Leptin labelling in pancreas was performed as previously described in Chapter 1. Rabbit polyclonal leptin antibody (Abcam, USA) was used for probing leptin (1:250 dilutions; 0.2µg.ml stock) and donkey anti-rabbit FITC was used as secondary.

Adipose mRNA expression of PPAR- α : RNA isolation and semiquantitative PCR was carried out as previously described in Chapter 1. Primer sequence for PPAR- α is as follows:

Sr.no	Gene of Interest	Primer sequence 5'-3'	Tm°C
1	Peroxisome proliferator activated receptor gamma (Amplicon size:576 bp)	Sense : TTCGATCCGTAGAAGCCGTG Antisense: CTAATACAAGTCCTTG TAGAT	61
2	Beta-Actin (Amplicon size: 240bp) House keeping gene	Sense : TCACCCACACTGTGCCCCATCTACGA Antisense: CAGCGGAACCGCTCATTGCCAATGG	60

Results:-

Body weight, Food intake (Table 1) and adiposity (Fig. 1):

Initial, final and body weight gain in control and experimental animals is shown in Table 1. Significant increment is seen in the final body weight and weight gain in high fat diet fed animals, which lowered significantly in 3% OI treated animals. Significant decrement is observed in the food intake in diabetic animals. Significant increment is seen in visceral adiposity as well the size of adipocytes in HFD fed mice. Treatment with 3% OI extract showed significant lowering of adiposity (Fig. 1).

Plasma lipid profile (Fig. 2-5):

Plasma cholesterol (Fig. 2), triglyceride (Fig. 3) and free fatty acids (Fig. 5) were all increased significantly in High fat diet (HFD) fed mice and the increase was to the tune of 3-5 times. There was also a concomitant reduction in HDL level (Fig. 4) by more than 50%. Extract supplemented rats showed significant reduction in cholesterol, triglyceride and free fatty acid levels. Plasma HDL showed significant increment from the very low diabetic level.

Plasma leptin levels (Fig. 6):

Leptin level (Fig. 6) was significantly increased in HFD fed diabetic mice while OI extract supplemented diabetic rats showed significant reversal of hormone levels towards non-diabetic levels.

Leptin immunostaining (Fig.7):

Intraislet leptin localization in pancreas of diabetic mice demonstrated higher leptin⁺ cells whereas OI extracted supplemented animals displayed lesser expression

PPAR γ expression (Fig. 8):

PPAR γ mRNA was significantly decreased in HFD fed diabetic mice. Though OI extract supplementation showed slight improvement in PPAR γ mRNA level, was however statistically insignificant.

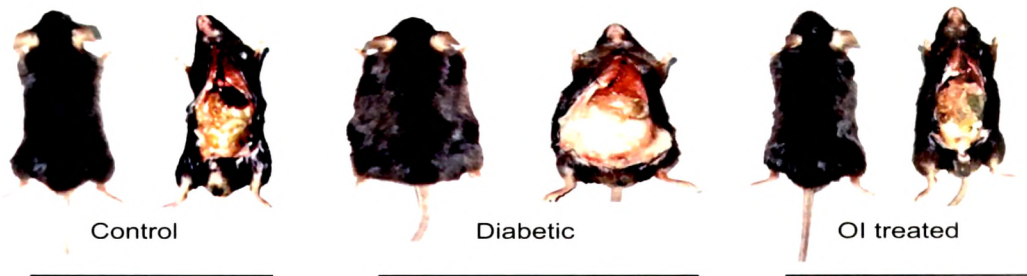
Table 1. Body weight and food intake in control and experimental animals.

	Control	Diabetic	OI treated
Body weight initial (gm)	24.2 ± 0.23	23.7 ± 0.41	22.6 ± 0.78
Body weight final (gm)	26.1 ± 0.43	41.3 ± 1.81 [♦]	29.3 ± 0.48 ^δ
Weight gain (gm)	1.9 ± 0.37	17.6 ± 0.67 [♦]	6.7 ± 0.32 ^{♦δ}
Food intake (gm/day/mice)	2.6 ± 0.17	1.87 ± 0.13 [•]	2.2 ± 0.18

•= p<0.01, ■=p<0.001, ♦=p<0.0001: Experimental groups compared to control

α= p<0.01, β= p<0.001, δ= p<0.0001: OI treated group compared to diabetic group

Fig. 1. Control, diabetic and OI extract treated mice opened to expose the viscera to show the variation in visceral adiposity.



Histomicrograph of sections of adipose tissue from control (a), diabetic (b) and OI extract treated (c) mice to depict difference in adipocyte dimensions. Scale bar represents 100µm. Magnification 450X.

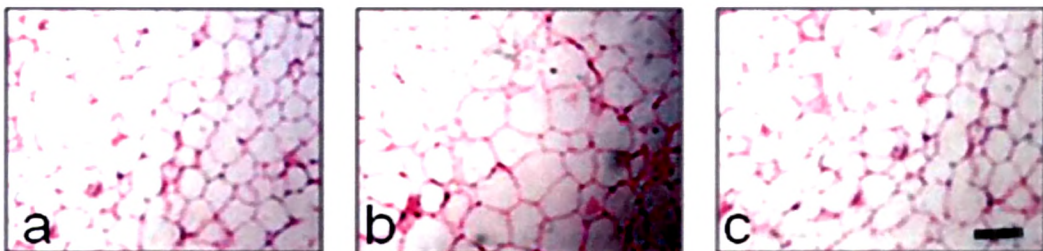
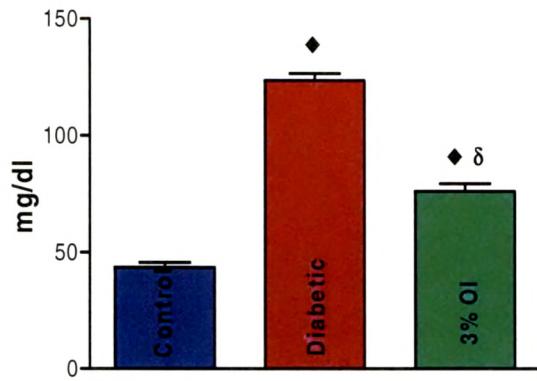
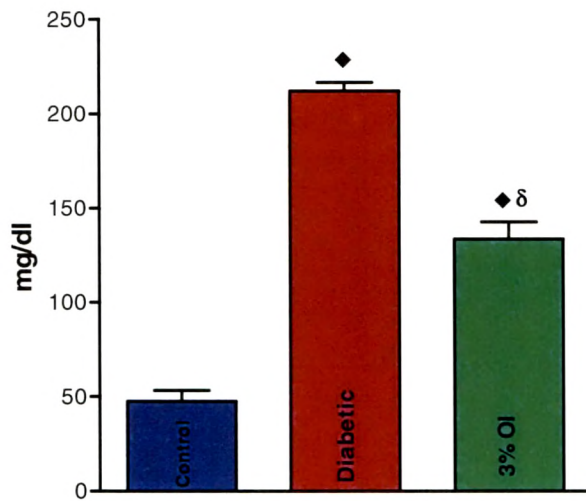


Fig. 2. Effect of 3% O I extract on Plasma cholesterol level in control and experimental animals



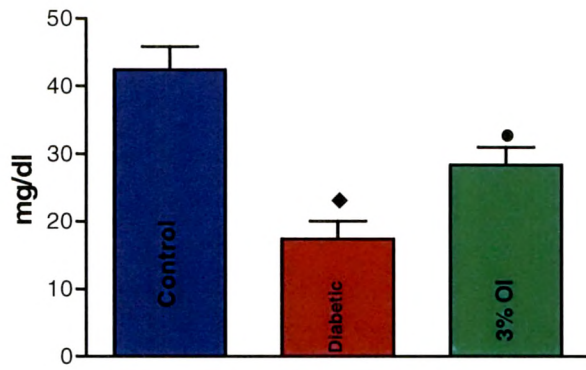
●=p<0.01, ■=p<0.001, ◆=p<0.0001: Experimental groups compared to control
α=p<0.01, β=p<0.001, δ=p<0.0001: 3% OI treated group compared with diabetic group

Fig. 3. Effect of 3% O I extract on Plasma TG level in control and experimental animals



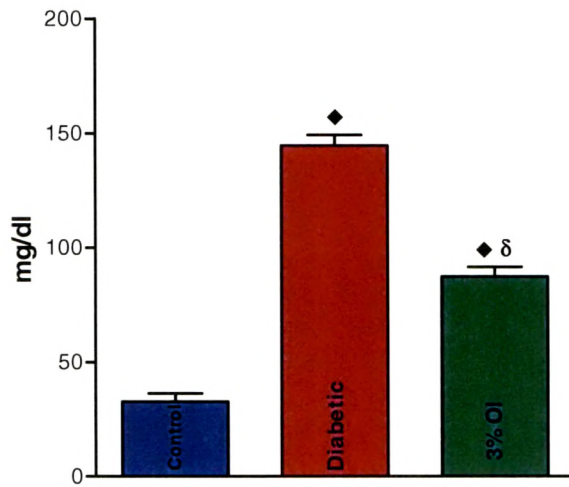
●=p<0.01, ■=p<0.001, ◆=p<0.0001: Experimental groups compared to control
α=p<0.01, β=p<0.001, δ=p<0.0001: 3% OI treated group compared with diabetic group

Fig. 4. Effect of 3% O I extract on Plasma HDL-C level in control and experimental animals



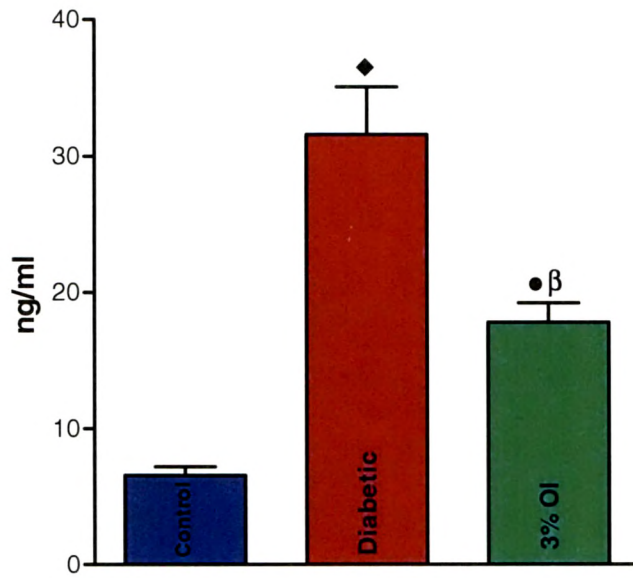
●=p<0.01, ■=p<0.001, ◆=p<0.0001: Experimental groups compared to control
α=p<0.01, β=p<0.001, δ=p<0.0001: 3% OI treated group compared with diabetic group

Fig. 5. Effect of 3% O I extract on Plasma FFA level in control and experimental animals



●=p<0.01, ■=p<0.001, ◆=p<0.0001: Experimental groups compared to control
α=p<0.01, β=p<0.001, δ=p<0.0001: 3% OI treated group compared with diabetic group

Fig. 6. Effect of 3% O I extract on Plasma Leptin level in control and experimental animals



●=p<0.01, ■=p<0.001, ◆=p<0.0001: Experimental groups compared to control
α=p<0.01, β=p<0.001, δ=p<0.0001: 3% OI treated group compared with diabetic group

IMMUNOSTAINING AND CONFOCAL MICROSCOPY

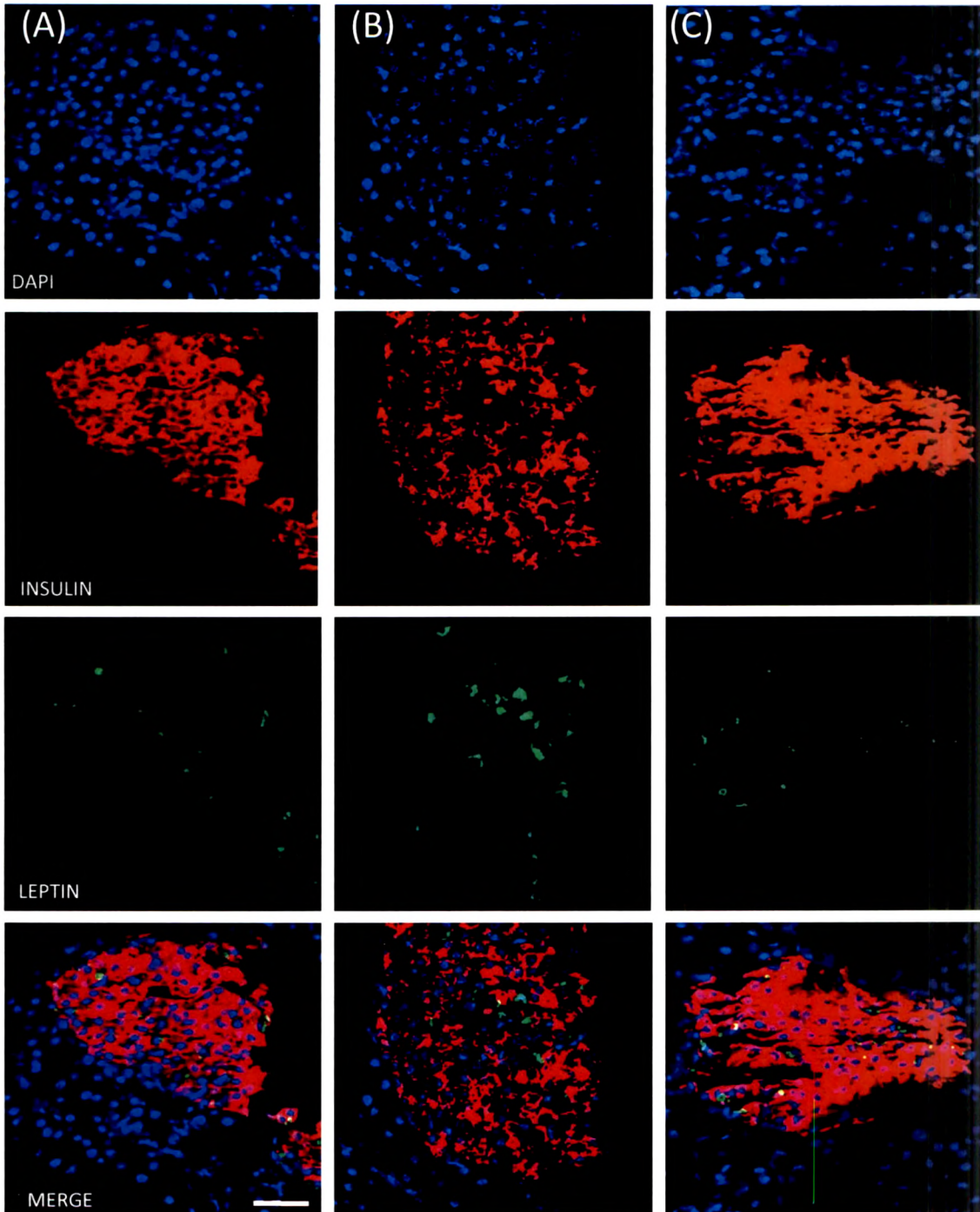
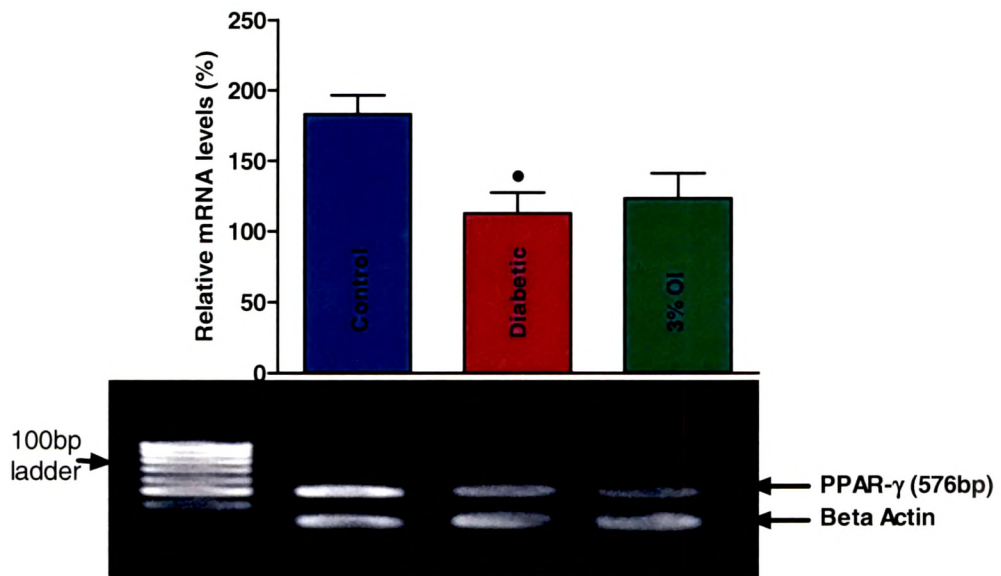


Figure 7: Images represent immunostained section of pancreas of A) Control, B) Diabetic, C) Diabetic + OI 3%. Guinea Pig anti insulin (red) and Rabbit leptin (green) were used as primary antibodies while Donkey-anti-GP-IgG-TRITC and Donkey-anti-rabbit-IgG-FITC as secondaries. DAPI (Blue) was used to visualize nuclei. The slides were visualized by Laser Scanning Confocal Microscope (LSM 510 META, ZEISS, Germany). Optical slices were taken at $\sim 0.8\mu\text{m}$. Laser gains, pin hole setting and magnification were set identical across samples. Scale bar represents $50\mu\text{m}$.

Fig.8. Effect of 3% OI extract on Plasma PPAR γ level in control and experimental animals



•=p<0.01, ■=p<0.001, ◆=p<0.0001: Experimental groups compared to control
 α =p<0.01, β =p<0.001, δ =p<0.0001: 3% OI treated group compared with diabetic group

Discussion:-

This investigation clearly projects diet induced T2D alterations in the form of increased body weight, greater feed efficiency, adiposity, dyslipidemia, hypoinsulinemia, hyperleptinemia, increased immunoreactivity for leptin in pancreatic acini and reduced PPAR γ expression in adipose tissue of BL 6 mice. Except for PPAR γ expression, all other alterations are reversed to a greater extent by OI extract supplementation.

Dyslipidemia as a feature of type 2 diabetes manifestation is by now well recognised and in the present study, both plasma FFA and TG are significantly increased in diabetic mice. The herein observed hypoinsulinemia in BL 6 diabetic mice does not only suggest the setting in of type 2 diabetes by 24 weeks of HFD but also of a situation of decreased glucose uptake and increased adipose tissue lipolysis, which contributes to hyperglycemia (Chapter 3a) and elevated serum FFA. The increased serum glycerol derived from lipolysis feeds the gluconeogenic pathway contributing to increased glucose production from liver while, the concurrent higher FFA level impairs insulin mediated glucose uptake, further contributing to serum glucose build up (chapter 3a). Free flow of fatty acids into liver in the diabetic state results in their conversion to triglycerides and phospholipids that get secreted as VLDLs or ketone bodies.

Apparently, upregulated activities of TG synthetic enzymes such as glycerol-phosphate acyl transferase, acyl glycerol-phosphate acyl transferase, phosphatidate phosphohydrolase acyl co-enzyme A: diacyl glycerol acyl transferase are to be expected in diet induced conditions of type 2 diabetes, obesity and metabolic syndrome. Similar increase in plasma FFA and hepatic TG and phosphatidate

phosphohydrolase has been reported by others as well in type 2 diabetes and obesity (Memon *et al.*, 1994; Cha *et al.*, 2001; Jung *et al.*, 2006).

It is possible to derive a strong correlation between resistance to insulin induced glucose uptake, VLDL-TG secretion rate and plasma TG level as has been discussed by Reaven (1991). Lipoprotein lipase of endothelial lining of capillaries release TGs from VLDL facilitating its uptake for energy generation or storage. Insulin being a cofactor along with apo C-II in VLDL breakdown, insulin deficiency in diabetic rats impairs this process and results in hypertriglyceredemia as evident herein, a strong risk factor for cardiovascular complications (Austin *et al.*, 1998; Goldberg, 2001; Aguilar-Salinos *et al.*, 2004; Pejis and Lee 2006). Although LDL level is increased in type 2 diabetic animals and individuals and its formation from VLDL in blood vessels is feasible, its direct role in cardiovascular disorders has been debatable (Goldberg, 2001; Nicholls *et al.*, 2010). In this context, the presently recorded hypertriglyceredemia together with the significantly lowered HDL seem to be potent markers of type 2 diabetes (Assmann and Schultze, 1998; Aguilar-Salinas *et al.*, 2004). Increased activity of CEPT (cholesterol ester transfer protein) or decreased activity of LCAT (lecithin cholesterol acyl transferase) could be the main defect in type 2 diabetes leading to decreased HDLs (Goldberg, 2001).

Dyslipidemia of C57BL6/J mice in the present study is also marked by significant hypercholesterolemia. Though most of the tissues are endowed with the ability of cholesterol metabolism, liver is the principal organ of cholesterol metabolism with the net amount of cholesterol being balanced by the rate limiting enzyme of cholesterol biosynthesis, HMG CoA reductase and the catabolic enzyme cholesterol 7 α -hydroxylase, which convert it into bile acids. Another enzyme that regulates intra hepatic free cholesterol level is acyl coenzyme A: cholesterol acyl

transferase (ACAT 2) that catalyzes the esterification of cholesterol for storage. Also involved in maintaining cholesterol balance is low density lipoprotein receptor (LDL-R), the primary pathway of LDL clearance from plasma. Differential alterations of all these key modulators of cholesterol balance in the body have been reported in conditions of hypercholesterolemia induced by high fat diet (HFD), high fat –high sugar diet (HFS) and nephrotic syndrome (Liu *et al.*, 1997; Vidon *et al.*, 2001; Way *et al.*, 2001; Vaziri, 2003; Roberts *et al.*, 2004). The general consensus of opinion from the above reports regarding HFD induced hypercholesterolemia is a down regulation of HMG CoA reductase (Vaziri and Liang, 1995) and up regulation of cholesterol α hydroxylase (Horton *et al.*, 1995; Cheema *et al.*, 1997). In view of the high intracellular free cholesterol content in the hepatic tissue of HFD rats, it is presumable that, there will be no defect in LDL-R or if at all there may be a slight over expression (Liu *et al.*, 1997) and, a down regulation of ACAT-2. All of these or some of these defects could account for the observed hypercholesterolemia in HFD fed C57BL 6/J mice in the present study.

The HFD mice are also characterized by a tremendous increase in serum leptin level and marked down regulation of adipose PPAR γ mRNA expression. The high level of leptin not only indicates increased adipose mass but also insulin resistance and β -cell dysfunctioning. Since PPAR γ is a down regulator of resistin gene expression in adipose tissue, the herein observed decreased PPAR γ mRNA in HFD mice suggest diet/ type 2 diabetes induced increase in resistin level (Steppan, 2001; Hangen *et al.*, 2001). This contention is supported by a recent study of Ahmed *et al.* (2010) in nicotinamide-streptozotocin induced diabetic rats. Since PPAR γ is a transcriptional regulator of adipogenesis and resistin an adipogenesis inhibitor favouring adipocytic differentiation (Caja *et al.*, 2005; Kusminski *et al.*, 2005), the

down regulated PPAR γ mRNA together with increased resistin may indicate a regulatory mechanism controlling adipose tissue mass. The increased leptin level together with the invoked hypoinsulinemia and insulin resistance stand to prevent reduced glucose intake and adipogenesis in WAT and drive visceral organ steatogenesis (liver, muscle etc) and augmented gluconeogenesis in keeping with the role of hepatic insulin resistance for resistin (Ukkola, 2002; Rajala *et al.*, 2004; Singhal *et al.*, 2007; Liu *et al.*, 2008). The interrelationships between leptin, insulin, resistin and glucose seem to be highly variant based on the strain of rats, dietary protocol and type 1 Vs type 2 diabetes. Even the genetic background and maintenance in different laboratories also make the response of C57 BL/6J mice seem to induce differential alterations, thereby preventing a pan-unitary interpretation (Trayhurn and Beattie, 2001; Hayamizu *et al.*, 2003; Asensio *et al.*, 2004; Lee *et al.*, 2006; Ahmed *et al.*, 2010 and other citations made earlier on dyslipidemia and resistin). The findings from the BL 6 mice maintained at Hyderabad (India) seem to respond to 24 week of HFD by hyperleptinemia, elevated resistin level and hypoinsulinemia. Though most of the studies mentioned above have documented parallel hyperleptinemia and hyperinsulinemia, the present study shows hypoinsulinemia which is well corroborated by the documented attenuated insulin immunoreactivity in pancreatic islets along with increased immunoreactivity for leptin. Hypoinsulinemia clearly suggests the setting in of type 2 diabetes and β -cell decompensation subsequent to islet compensation during prevailing insulin resistance. Apparently, the genetic breed maintained in this geographical location progresses to type 2 diabetes stage by 24 week of HFD when feeding was started in the immediate post-weaning age (4-5 weeks). Lack of uniformity in the age at which HFD is initiated, the duration of dietary feeding, the fat composition of diet and the genetic makeup, all seem to

contribute to variability in response and hence caution is to be exercised while interpreting the results.

In the present study, by 24 weeks of HFD, the C57BL6/J mice have entered into type 2 diabetic stage with islet decompensation. Islet decompensation could be marked by increased dysfunctioning or destruction of β -cells reflected in the marked hypoinsulinemia. The observed loss of insulin immunoreactivity and increase in leptin immunoreactivity tend to suggest a paracrine inhibitory influence of intra-islet leptin on β -cell functioning and insulin production in HFD fed BL 6 mice. There are many reports in recent times alluding to an inhibitory role of leptin on β -cell insulin secretion, though the reciprocal/ bidirectional feedback system between insulin and leptin suggested by Reddy *et al.*, (2004) is not supported in the present observations (Covey *et al.*, 2006; Tuduri *et al.*, 2009; Park *et al.*, 2010).

Beta-cell decompensation by way of either dysfunctioning or β -cell destruction is also a direct consequence of gluco and/or lipotoxicity. In this connection, lipid overload and increase in free fatty acids are known to cause β -cell destruction (Unger and Zhou, 2001; Donath *et al.*, 2005). Different mechanisms have been proposed for gluco/ lipotoxicity and leptin induced β -cell failure/destruction such as both glucotoxicity and lipotoxicity converging towards generation of effectors on β -cell function (Poitont and Robertson, 2002) such as disordered mitochondrial function, TG/ FFA cycling, AMPK/ malonylCoA signalling, ER stress and compensatory β -cell growth (Prentki and Nolan, 2006), decreased leptin sensitivity of β -cells (Morioka *et al.*, 2007), leptin inhibition of β -cell secretion either directly or indirectly through decreased osteocalcin activity (Hinoi *et al.*, 2008) and glucotoxicity and leptin inducing β -cell apoptosis by activated JNK and increased caspase activity (Maedler *et al.*, 2008).

Supplementation of HFD diet with OI extract significantly prevented augmented body weight gain, reduced adipocyte size, serum lipid profile and serum and islet leptin level and showed no effect on adipose PPAR γ mRNA expression. The protective effect of OI on insulin level is well reflected in the glycemic status of these rats (Ansurallah *et al.*, 2010). The attenuated glycemic status indicating better insulin sensitivity is corroborated by the herein observed minimal elevation in serum lipid fractions and reduced visceral adipose mass. The lower WAT mass in HFD + OI mice signify the anti-adipogenic actions of the extract in resisting the adipogenic potential of HFD. Maximal beneficial effect seems to be on plasma cholesterol as seen by the maximal resistance against the hypercholesterolemic action of HFD. Resistance towards elevation in TG and FFA and decline in HDL is almost to the same degree though the protective action against HDL is relatively better. The TG/HDL ratio is also almost 3 times lesser in HFD + OI mice compared to HFD alone mice. The protective effect of OI against plasma triglyceride and total cholesterol elevation could be related with the insulinogenic action of the principles in OI as, an insulin secretagogue effect of the extract has been documented under *in vitro* conditions (Chapter 4). This insulin secretagogue effect of OI extract may be related with its high flavonoid content as, flavonoids have been shown to have insulin secretion elevating activity (Hii and Howell, 1985; Ahmed *et al.*, 2010). Recently, lipid lowering efficacy of flavonoids has been adequately documented in hypercholesterolemic subjects (Jung *et al.*, 2003). Such an action has also been demonstrated in HFD induced type 2 diabetic mice (Jung *et al.*, 2006). The anti-hypercholesterolemic action of flavonoids has been related with their ability to lower hepatic HMG-CoA reductase and ACAT activities with increase in fecal cholesterol and also on possible intestinal anti-absorptive effect (Park *et al.*, 2002; Raz *et al.*,

2005; Jung *et al.*, 2006; Ahmed *et al.*, 2010). Though a down regulation of hepatic HMG-CoA reductase activity is presumed in HFD mice due to higher dietary supply of cholesterol and increased hepatic free cholesterol content, it is likely that, the active principles of OI extract may mediate further down regulation of HMG-CoA reductase to facilitate lowering of plasma cholesterol load.

The present observations also tend to support an anti-triglyceridemic and free fatty acid lowering effect of the principles in OI extract. A possible mechanism in this context could be lowered triglyceride synthesis. In this connection, flavonoids have been shown to have significant down regulative action on glucose-6-phosphate dehydrogenase and phosphatidate phosphohydrolase activities (rate limiting enzymes of triglyceride synthesis) as has been shown by Cha *et al.* (2001) and Jung *et al.* (2006). Decreased hepatic fatty acid synthesis and lowered triglyceride production are also likely to reflect on plasma triglyceride level by modulating the hepatic formation of VLDL (Windmueller and Spaeth, 1967). The possibility of OI extract exerting an insulinomimetic action cannot be ruled out as Borradiule *et al.* (2003) have corroborated LDL-R expression and inhibited apo B secretion in Hep G₂ cells as possibility due to insulin like effects of navingen, a flavonoid. Another mechanism for lowering plasma TG and FFA levels could be down regulated hepatic fatty acid synthetase and G6PDH activities, which could render availability of long chain fatty acids for triglyceride synthesis at a premium (Halminski *et al.*, 1991; Jung *et al.*, 2006).

Many studies have shown decreased adipose tissue PPAR γ expression upon feeding of C57BL6/J mice with HFD and increased expression with flavonoids or flavonoid containing extracts (Kim *et al.*, 2004; Jung *et al.*, 2006; Shih *et al.*, 2008; Ahmed *et al.*, 2010). Number of functions have been ascribed to PPAR γ like,

promoting pre-adipocyte differentiation, stimulation of storage of fatty acids, increase insulin sensitivity by channelizing fatty acids into adipose tissue thereby decreasing plasma FFA and alleviation of lipotoxicity and by decreasing hepatic triglyceride content, activation of glucokinase and inhibition of HMG-CoA reductase (Fulgencio *et al.*, 1995; Wilson *et al.*, 2000, Yamauchi *et al.*, 2001; Hevener *et al.*, 2003; Lee *et al.*, 2003; Kim *et al.*, 2004; Anandharajan *et al.*, 2005; Staels and Fruchart, 2005; Feige *et al.*, 2006; Jung *et al.*, 2006; Lefebvre *et al.*, 2006; Ahmed *et al.*, 2010). As against these reports of increased PPAR γ expression with flavonoids or extracts, the present study has failed to prevent the down regulation of PPAR γ induced by HFD. Despite the lower PPAR γ expression in HFD + OI mice, it is interesting to note that, OI extract is successful in resisting dyslipidemia and hyperglycemia. Apparently, the OI extract used in the present study has principles which is / are able to increase insulin level and sensitivity and decrease gluconeogenesis and glucokinase mediated hepatic glucose uptake and oxidation as well as promote glucose transport into muscle (Chapter 3 a, b). The anti-hyperleptinemic effect of OI extract by modulating the leptin level may not only prevent insulin resistance but, also by its protective effect against increased leptin expression in pancreatic islets induced by HFD, may also contribute to robust β -cell functioning and insulin production. It is also likely that some unknown principles in OI extract may also act at downstream sites of PPAR γ signalling pathways in liver and adipose tissue and mediate PPAR γ mediated actions without an actual increase in PPAR γ expression. More detailed analysis of OI extract to identify the active principles and their mode of action would be very rewarding in the development of novel therapeutics against HFD induced glucose dyshomeostasis and dyslipidemia.

Since type 2 diabetes is a complex metabolic disorder affecting multiple loci like hyperglycemia, impaired insulin action/ secretion, dyslipidemia etc. and has complicated expression patterns by multiple genetic background and varied interactions with environmental conditions, its ameliorative or therapeutic intervention need to address to all the above multifaceted manifestations. Since most of the standard drug therapies are beset with secondary and other complications, herbal therapies capable of acting at multiple loci for a comprehensive effect need to be developed.